Temperature Specific Regulation of NDR Kinase Orb6 by MAP kinase Sty1 to Promote Heat Stress Resilience

Laura P. Doyle[1], Robert N. Tams[1], Chuan Chen[1], Illyce Nuñez[1], Patrick Roman Haller[1], Fulvia Verde[1**]

Author Affiliations: [1]Department of Molecular and Cellular Pharmacology, University of Miami, Miami, FL.

Keywords (max. 6): NDR kinase Orb6; MAP kinase Sty1; Cdc42 GTPase; Sts5 RNP granule assembly; heat stress; *Schizosaccharomyces pombe*

Abstract

Cellular response to environmental fluctuations, such as increased temperature, is crucial in promoting cell survival and plays an increasingly recognized role in cancer biology. Important cellular functions altered by heat stress are cell polarization and protein translation. Previous studies have shown that heat stress alters the dynamics of Cdc42, a key regulator of cell polarization in eukaryotes, and promotes RNP granule formation, reprogramming protein translation. The biological mechanisms underlying these vast changes are only partially known. Here, we report that conserved NDR kinase Orb6, a homologue of mammalian STK38, responds to heat stress and regulates heat stress resilience by modulating Cdc42 dynamics and promoting stress granule assembly. Also, we discovered a finely tuned mechanism whereby stress-activated MAP kinase Sty1 negatively regulates Orb6 kinase and Orb6 C-terminal phosphorylation during heat stress. Orb6 inhibition by Sty1 increases the sensitivity of the cell to heat stress in a temperature-specific manner, fostering increased stress resilience and metabolic adaptation. These observations highlight the role of NDR kinase in the process of heat adaptation and thermotolerance during environmental cell exposure to elevated temperatures.

Summary statement

Nuclear Dbf2-related kinase Orb6 inhibition by stress-activated protein kinase Sty1 promotes heat stress resilience in a temperature specific manner.

37 **Introduction**

38 The ability to respond to varying environmental conditions, such as elevated
39 temperature, is a vital cellular defense mechanism that promotes adaptation and survival
40 (Zayani *et al.*, 2025). Heat stress response activates adaptive mechanisms including
41 antioxidant defenses, metabolic shifts, and heat shock proteins (HSPs) induction (Jung
42 *et al.*, 2013; Gomez-Pastor, Burchfiel and Thiele, 2018; Ciocca, Arrigo and Calderwood,
43 2013; Hu *et al.*, 2022; Ding and Gao, 2025). Activation of the heat shock response usually
44 provides cytoprotective effects, and HSPs have been found to promote survival of cancer
45 cells (Wu *et al.*, 2017). An increase in HSP levels has also been found in chronic
46 inflammatory conditions such as rheumatoid arthritis (Fouani *et al.*, 2022). In eukaryotes,
47 severe heat stress (typically ≥ 42°C) rapidly disrupts cellular function, triggering a robust
48 heat shock response, protein denaturation and aggregation, as well as a decrease in
49 protein synthesis.

50 During heat stress, cells undergo distinct morphological changes. Mammalian cells
51 often lose their spread morphology and become more rounded due to cytoskeletal
52 reorganization (Velichko *et al.*, 2013; Dressler *et al.*, 2005; Gungor *et al.*, 2014). However,
53 the mechanisms that regulate morphological changes during heat stress are poorly
54 understood. In the fission yeast *Schizosaccharomyces pombe*, an amenable model
55 system, mild, sublethal heat stress at 36°C alters cell polarization and the dynamic
56 behavior of Cdc42 GTPase (Vjestica *et al.*, 2013), a key regulator of cell morphology in
57 eukaryotes (Schwamborn and Püschel, 2004; Stankiewicz and Linseman, 2014). In
58 unstressed conditions, Cdc42 displays oscillatory dynamics at cell tips (Das *et al.*, 2012).
59 During heat stress (Vjestica *et al.*, 2013) as well as in response to different environmental

60 conditions such as pheromone exposure (Bendezú and Martin, 2013), oxidative stress
61 (Salat-Canela *et al.*, 2021), or nitrogen starvation (Chen *et al.*, 2019), an alternative
62 "exploratory" pattern of Cdc42 emerges, where dynamic patches of active Cdc42 appear
63 and disappear throughout the cell membrane. While the emergence of exploratory Cdc42
64 dynamic involves the activation of the conserved stress-activated MAP kinase Sty1/Spc1
65 (Salat-Canela *et al.*, 2021; Mutavchiev, Leda and Sawin, 2016; Doyle *et al.*, 2025), the
66 mechanism that regulates Cdc42 dynamics shift during thermal stress is insofar poorly
67 understood.

68 During heat stress, cells also rapidly suppress global protein synthesis to
69 conserve energy and prevent accumulation of misfolded protein by the inhibition of
70 translation initiation and mRNA sequestration into stress granules and P-bodies for
71 storage or decay (Kedersha *et al.*, 2005; Grousl *et al.*, 2009). Stress granules (SGs) are
72 membraneless cytoplasmic aggregates that form in response to various stress conditions,
73 including heat shock, oxidative stress, osmotic stress, and infections (Marcelo *et al.*,
74 2021)**.** Their primary role is to protect mRNA and regulate translation during stress,
75 helping cells survive adverse conditions. The formation process relies on liquid–liquid
76 phase separation (LLPS), driven by multivalent interactions between RNA-binding
77 proteins (RBPs) and untranslated mRNAs. Stress granules are critical adaptive structures
78 that integrate translational control with cellular stress signaling (Desai *et al.*, 2026).
79 Dysregulation of SG dynamics is increasingly recognized as a contributor to human
80 disease, and is strongly linked to neurodegeneration (ALS, FTD), cancer and viral
81 infections (Ramaswami, Taylor and Parker, 2013; Anderson, Kedersha and Ivanov, 2015;
82 Aguzzi and Altmeyer, 2016; Gilks *et al.*, 2004; Alberti and Dormann, 2019).

83 Nuclear Dbf2-related (NDR) kinases are highly conserved members of the AGC
84 protein kinase family which regulate essential cellular processes including
85 morphogenesis, growth and proliferation, mitosis, and apoptosis (Hergovich *et al.*, 2006;
86 Cornils *et al.*, 2011; Yang *et al.*, 2014; Vichalkovski *et al.*, 2008; Verde, Mata and Nurse,
87 1995; Chiba *et al.*, 2009; Hergovich *et al.*, 2007; Hergovich *et al.*, 2009; Verde, Wiley and
88 Nurse, 1998). Several studies have implicated dysregulation of NDR kinases in the
89 development of cancer, and NDR also plays a role in neuronal differentiation (Adeyinka
90 *et al.*, 2002; Millward *et al.*, 1998; Hauschild *et al.*, 1999; Ross *et al.*, 2000; Cornils *et al.*,
91 2010; Zhang *et al.*, 2015; Napoletano *et al.*, 2011). The fission yeast *S. pombe* has a
92 NDR/LATS kinase known as Orb6, which is responsible for regulation of polarized cell
93 growth (Verde, Mata and Nurse, 1995). We previously reported that Orb6 kinase has
94 separate roles in the control of Cdc42 GTPase (Das *et al.*, 2015; Das *et al.*, 2009), and
95 mRNA translation (Nunez *et al.*, 2016; Chen *et al.*, 2019). Orb6 governs cell polarity by
96 promoting the Ras1-dependent Cdc42 control axis (Chen *et al.*, 2019) and by inhibiting a
97 stress-activated Cdc42 module (Doyle *et al.*, 2025; Salat-Canela *et al.*, 2021) composed
98 of the guanine nucleotide exchange factor Gef1 (Das *et al.*, 2015; Das *et al.*, 2012; Das
99 *et al.*, 2009; Coll *et al.*, 2003) and the Cdc42 GAP (GTPase Activating Protein) Rga3
100 (Doyle *et al.*, 2025; Gallo Castro and Martin, 2018). Downregulation of Orb6 kinase, which
101 suppresses Ras1 GTPase and derepresses the stress-activated Cdc42 module, leads to
102 the emergence of Cdc42 exploratory dynamics (Chen *et al.*, 2019; Das *et al.*, 2009).
103 Orb6 kinase also promotes polarized cell growth by spatiotemporal regulation of
104 RNA-binding protein Sts5 (Nunez *et al.*, 2016; Chen *et al.*, 2019). Sts5 is an RNA binding
105 protein (RBP) homologous to human Dis3L2, which is associated with Perlman's

106 syndrome and Wilm's tumor in humans (Astuti *et al.*, 2012; Lv *et al.*, 2015; Robinson *et*
107 *al.*, 2015; Malecki *et al.*, 2013; Toda *et al.*, 1996; Vaggi *et al.*, 2012; Jansen *et al.*, 2009;
108 Kurischko *et al.*, 2011). Sts5 functions to repress translation of specific mRNAs, many of
109 which encode proteins involved in polarized cell growth, via binding and sequestration
110 into ribonucleoprotein (RNP) granules (Nunez *et al.*, 2016), under conditions of nutritional
111 stress (Nunez *et al.*, 2016; Chen *et al.*, 2019; Magliozzi and Moseley, 2021).
112 Environmental stress such as nitrogen starvation, or crowded growth conditions leading
113 to stationary phase, inhibit Orb6 kinase activity, which results in the translational
114 repression of mRNAs involved in polarized growth via formation of Sts5 granules (Nunez
115 *et al.*, 2016; Chen *et al.*, 2019).

116 In this paper, we report that heat stress downregulates Orb6 kinase activity,
117 promoting Cdc42 exploratory dynamics and Sts5 coalescence into stress granules.
118 Further, we find that Orb6 kinase inhibition increases stress granule formation and
119 promotes cell resilience to heat stress. Recently, we reported that stress activated MAP
120 kinase Sty1 negatively regulates Orb6 kinase activity during nitrogen starvation (Doyle *et*
121 *al.*, 2025). In this paper, we show that MAP kinase Sty1 has also a role in the induction
122 of exploratory Cdc42 dynamics, Sts5 granule assembly, and the inhibition of Orb6 kinase
123 activity during mild heat stress. Furthermore, we find that the levels of phosphorylation of
124 Orb6-Thr456, the C-terminal hydrophobic motif, are decreased upon heat stress and that
125 Sty1 activation enhances the sensitivity of Thr456 phosphorylation and Orb6 kinase
126 function to heat stress. Thus, our observations identify a temperature specific regulation
127 of NDR kinase Orb6 by MAP kinase Sty1 to promote exploratory Cdc42 dynamics and
128 stress resilience.

129 **Results**

130

131 **Orb6 kinase function and activity are downregulated by heat stress.**

132 We have previously shown that Orb6 kinase is sensitive to nutritional stress, and
133 that downregulation of Orb6 kinase activity alters cell morphology and protein translation
134 during nitrogen deprivation (Chen *et al.*, 2019). During nutritional stress, Orb6 kinase
135 activity decreases and therefore phosphorylation of the Cdc42 control factors and Orb6
136 substrates Gef1 (Cdc42 GEF) and Rga3 (Cdc42 GAP) declines, promoting exploratory
137 Cdc42 dynamics (Das *et al.*, 2015; Chen *et al.*, 2019; Doyle *et al.*, 2025). The onset of
138 exploratory Cdc42 dynamics and increased Gef1 membrane localization were previously
139 reported to occur also during exposure to sublethal mild heat stress at 36°C (Vjestica *et*
140 *al.*, 2013). Therefore, we investigated if Orb6 kinase has a role in the cellular response to
141 heat stress. Consistent with previous findings, we found that Gef1-3YFP localizes to the
142 cell membrane after 30 minutes at 36°C (Fig. 1A, B) as compared to the control which
143 remained at 25°C. Further, we found that Gef1-3YFP also localizes to the cell membrane
144 at the higher, severe heat stress temperature of 42°C (Fig. 1A, B).

145 As Gef1 is a substrate that is phosphorylated by Orb6 at serine 112, we sought to
146 measure Orb6 activity using a previously described custom phospho-specific antibody for
147 Gef1-S112 (Chen *et al.*, 2019). We found that Gef1-S112 phosphorylation decreases
148 after 30 minutes at 36°C, a sublethal temperature that induces heat stress, and is further
149 exacerbated at 42°C, a lethal temperature that induces a severe heat shock response
150 (Fig. 1C,D). These results indicate the Orb6 activity decreases during both mild and
151 severe heat stress exposure, fostering exploratory Cdc42 dynamics.

152 During heat exposure, cells reorganize their RNA and protein metabolism by
153 forming two major types of cytoplasmic granules: Stress Granules (SGs) (Guzikowski,
154 Chen and Zid, 2019; Mahboubi and Stochaj, 2017), and Processing Bodies (P-bodies).
155 Both are membraneless organelles formed by liquid–liquid phase separation, but they
156 have distinct roles and compositions. We previously demonstrated that Orb6 kinase
157 controls polarized cell growth and protein translation by phosphorylating the highly
158 conserved RNA binding protein Sts5. Sts5, an Orb6 substrate, remains diffused in the
159 cytoplasm when Orb6 is active, whereas it partially co-localizes with P-(Processing)
160 Bodies following Orb6 inhibition, or in media lacking glucose or nitrogen (Nunez *et al.*,
161 2016; Magliozzi and Moseley, 2021).

162 Consistent with Orb6 kinase activity being downregulated by heat exposure, we
163 found that Sts5-3YFP remains diffused in the cytoplasm at 25°C, whereas it forms puncta
164 at both 36°C and 42°C (Fig. 1E, F). We found that Sts5-3YFP puncta readily associate
165 with stress granules (using Pabp1-dsRed stress granule marker) at 42°C (Figure 1E,g-i,
166 1G), but not at 36°C where we find no stress granule assembly (Figure 1E,d-f, 1G).
167 Conversely, we find that Sts5-3YFP colocalizes with P-body marker Dcp1-mCherry at
168 both 36°C and 42°C (Fig. S1).

169 We sought to further confirm Sts5 and stress granule co-localization, under
170 conditions of glucose limitation, which strongly induces stress granules formation (Nilsson
171 and Sunnerhagen, 2011) as well as Sts5 aggregation into RNP granules (Nunez *et al.*,
172 2016). We investigated the localization of *ssp1* mRNA, a Sts5-bound mRNA which is
173 translationally repressed upon formation of Sts5 puncta (Nunez *et al.*, 2016) by RNA-
174 FISH analysis. *ssp1* encodes a CamK kinase (Hanyu *et al.*, 2009; Matsusaka *et al.*, 1995).

175 We observed co-localization of Sts5 puncta, *ssp1* mRNA, and stress granules in cells
176 cultured in medium lacking glucose (Fig. 2A). We previously used *ssp1* mRNA to detect
177 co-localization of Sts5 with P-bodies (Nuñez *et al.*, 2016) .
178 Overall, these findings show that Orb6 kinase activity is downregulated upon heat
179 stress and heat shock, fostering Cdc42 exploratory dynamics and coalescence of RNA
180 binding protein Sts5 into stress granules and P bodies.
181
182 **Orb6 inhibition and Sts5 Aggregation Promote Stress Granule Assembly.**
183 We have previously demonstrated that Orb6 inhibition promotes the formation of
184 P-Bodies in a Sts5 dependent manner (Nunez *et al.*, 2016), suggesting that Sts5
185 aggregates may promote P-Body formation during glucose starvation. To test whether
186 Sts5 plays a role in stress granule nucleation, we followed the formation of stress granules
187 in the *sts5Δ* mutant using the stress granule marker Pabp1-DsRed. In this particular
188 experiment, we induced stress granules via glucose deprivation, which strongly induces
189 stress granules assembly, facilitating quantification. We found that the number of stress
190 granules decreased by 44% in *sts5Δ* mutant cells as compared to control cells (Fig. 2B,
191 b, d; Fig. 2D) cultured for 20 minutes in media lacking glucose. In media containing
192 glucose, Pabp1-DsRed is largely diffuse within the cytoplasm in both the *sts5Δ* and
193 control strains (Fig. 2B; a, c).
194 To determine if inhibition of Orb6 kinase drives stress granule formation, we
195 treated *orb6-as2 pabp1-DsRed* cells with 1-NA-PP1 inhibitor and found that inhibition of
196 Orb6-as2 at 25°C does not induce stress granule formation (Fig. 2C; a, c), These findings
197 indicate that Orb6 kinase inhibition alone is not sufficient to induce stress granule

198 formation, while it is sufficient to promote P-Body formation, as we previously reported
199 (Nunez *et al.*, 2016). However, when 1-NA-PP1 treated cells were subsequently heat
200 shocked for 20 minutes at 42ºC, we observed a remarkable increase in the number of
201 stress granules, as compared to the heat shocked DMSO control (Fig. 2C; b, d). The
202 number of stress granules formed was quantified for three independent experiments
203 (n=90 cells/condition), and the number of stress granules increased, on average, by 54%
204 for the 1-NA-PP1 treated cells as compared to the heat shocked DMSO control (Fig. 2E).
205 Overall, these data indicate that the presence of Sts5 is important for the formation of
206 stress granules, and that Orb6 kinase plays a role in this process by modulating the extent
207 of stress granule formation.
208
209 **Sts5 aggregation Modulates Heat Resilience in *S. pombe.***
210 Stress granule formation provide a mechanism to protect cells from environmental stress
211 and promote cell survival (Mahboubi and Stochaj, 2017). These condensates can
212 modulate susceptibility to heat stress (Riback *et al.*, 2017; Kroschwald and Alberti, 2017).
213 Since Sts5 responds to heat by co-localizing with both stress granules and P-Bodies (Fig.
214 1E, Fig. S1) and is important for stress granule formation (Fig. 2B), we hypothesized that
215 modulating the assembly of Sts5 into RNP granules plays a role in cell protection from
216 heat stress. Sts5 contains an intrinsically disordered domain (IDD), which is
217 phosphorylated by Orb6 kinase at serine 86 (Chen *et al.*, 2019). Modification of Sts5
218 serine 86 to alanine promotes increased Sts5 puncta formation, increases cell resilience
219 during nutritional stress and promotes chronological lifespan extension (Chen *et al.*,
220 2019). Thus, we tested if loss of Sts5 (*sts5Δ*), or the presence of the *sts5-S86A* mutation

221 affect cell survival during extended heat stress or heat shock. To test the role of Sts5
222 during heat stress and in heat tolerance (exposure to heat for extended times), wild-type,
223 *sts5Δ*, *sts5-HA*, and *sts5-S86A-HA* log-phase cells were incubated for 6 hours at heat
224 stress temperature (36.5°C) or control temperature (25°C) in a shaking incubator and
225 plated to calculate colony forming units (CFUs) (see Methods). We found that the *sts5Δ*
226 strain exhibited decreased survival compared to wild-type (Fig. 3A). Conversely, the *sts5-*
227 *S86A-HA* strain displayed increased survival, as compared to the *sts5-HA* or wild-type
228 controls (Fig. 3A). The *sts5-HA* strain exhibited similar survival as compared to the wild
229 type, as expected. We previously established that addition of the *sts5-S86A* mutation
230 does not alter Sts5 protein levels (Chen *et al.*, 2019).

231 To test response upon acute heat shock, wild-type, *sts5Δ*, *sts5-HA*, and *sts5-*
232 *S86A-HA* strains were exposed to a 48ºC heat shock for 15 minutes. We found that the
233 *sts5Δ* strain exhibited decreased survival as compared to the wild-type control (Fig. 3B).
234 Again, the *sts5-S86A-HA* mutant exhibited increased survival as compared either the
235 wild-type or *sts5-HA* controls (Fig. 3B).

236 Thus, our data indicate that Sts5 coalescence is important for survival and heat
237 stress resilience following various durations and intensities of exposure to elevated
238 temperatures. Therefore, we tested whether Sts5 granule assembly is modulated by
239 increased temperature and whether the *sts5-S86A* mutation increases formation of Sts5
240 puncta following exposure to heat. To do this, *sts5-3xYFP* and *sts5-S86A-3xYFP* strains
241 were cultured at 29°C, 32°C, 35.5°C, or 42°C for 30 minutes, while control *sts5-3xYFP*
242 and *sts5-S86A-3xYFP* cells were maintained at 25°C throughout the experiment.
243 Following heat stress, fluorescence microscopy was performed and the number of Sts5

244 puncta were counted at each temperature. The *sts5-3xYFP* control began to form visible
245 puncta at 35.5°C (Fig. 3C; a-d), whereas the *sts5-S86A-3xYFP* mutant began to form
246 puncta already at 25°C (Fig. 3C, f-j). These differences were statistically significant (Fig.
247 3D), and *sts5-S86A* predisposition to the formation of puncta was readily apparent until
248 the temperature reached 42°C at which point the control formed approximately the same
249 number of puncta (Fig. 3Ce, Cj, 3D).

250 Our findings indicate an important role for serine 86 phosphorylation in modulating
251 the extent of Sts5 puncta assembly in response to increased temperatures (Fig. 3C, D).
252 Since Orb6 kinase phosphorylates serine 86 (Chen *et al.*, 2019), we tested if
253 downregulation of Orb6 kinase also increases cell resilience to heat stress. To
254 transcriptionally repress Orb6, a thiamine-repressible o*rb6-as2* strain was used. Log
255 phase wild-type and *orb6-as2* cells were grown with or without 15 μM thiamine for 16
256 hours at 32°C. Samples were diluted to an equivalent optical density and were heat
257 shocked at 48°C for 15 minutes while control samples were maintained at 32°C. The
258 *orb6-as2* strain, in the presence of thiamine, exhibited a striking increase in survival
259 following heat shock compared to the untreated control (Fig. 3E). This striking increase
260 in resilience was readily observed on Petri plates (Fig. S2) and was notably higher than
261 the relative increase in heat resilience observed for the *sts5-S86A* mutant (Fig. 3A-B).
262 Overall, these data indicate that the Orb6 kinase modulates stress granule assembly and
263 resilience to heat stress, in part, by phosphorylating mRNA binding protein Sts5 on serine
264 86.
265

266 **Conserved MAP kinase Sty1 negatively regulates Orb6 activity in a temperature**
267 **specific manner.**

268 The mitogen-activated protein kinase (MAPK) Sty1/Spc1 is activated upon
269 exposure to diverse stressors such as nitrogen starvation, osmotic changes, oxidative
270 stress, and heat shock (Toone and Jones, 1998; Shiozaki and Russell, 1996; Millar, Buck
271 and Wilkinson, 1995; Degols, Shiozaki and Russell, 1996). Recently, we have shown that
272 Sty1 activation during nitrogen starvation negatively regulates Orb6 activity (Doyle *et al.*,
273 2025). Therefore, we tested if Sty1 has a role in Orb6 regulation during heat stress, by
274 visualizing Sts5-3YFP aggregation during either mild or severe heat stress (36°C or 42°C)
275 for 30 minutes in the presence or absence of *sty1.* We find that upon loss of *sty1,* Sts5-
276 3YFP does not assemble into granules at 36°C but it still assembles into granules at 42°C
277 (Fig. 4A). The number of Sts5 granules per cell at 42°C is similar in both the presence or
278 absence of *sty1* (Fig. 4B). These results indicate that Sts5 granule assembly during heat
279 stress is dependent on the presence of Sty1 at 36°C but not at 42°C.

280 Previously, we have shown that Orb6 phosphorylates two regulators of Cdc42, a
281 GEF Gef1 (Das *et al.*, 2015) and a GTPase activating protein (GAP) Rga3 (Doyle *et al.*,
282 2025) to spatially regulate Cdc42 dynamics. When Orb6 is inhibited during nitrogen
283 starvation, Gef1 and Rga3 move to the cell membrane and facilitate the onset of
284 exploratory Cdc42 dynamics, where active Cdc42 forms dynamic patches along the cell
285 membrane (Doyle *et al.*, 2025). These exploratory Cdc42 dynamics are also found upon
286 different stress exposure, including heat stress at 36°C (Vjestica *et al.*, 2013). Thus, we
287 sought to investigate if exploratory Cdc42 dynamics were dependent on Sty1 upon heat
288 exposure. We visualized active Cdc42 using fluorescently tagged Cdc42-Rac Interactive

289 Binding domain bioreporter CRIB-GFP or the Cdc42 GEF Gef1 using Gef1-3YFP. We
290 find that exploratory Cdc42 dynamics and Gef1-3YFP membrane localization are induced
291 by heat exposure at 36°C and 42°C and that these effects are dependent on Sty1 at 36°C,
292 but not 42°C (Fig. 4C-F).

293 Further, we tested the effects of heat stress and heat shock on Gef1-S112
294 phosphorylation by Orb6 kinase, in the presence and absence of *sty1.* We find that Gef1-
295 S112 phosphorylation decreases upon exposure to 36°C and 42°C (Fig. 4G,H). In the
296 absence of *sty1,* we find that Gef1-S112 phosphorylation remains constant at 36°C but
297 decreases to similar levels as wild-type at 42°C (Fig. 4G, H). Sty1 activation in these
298 experimental conditions was validated by measuring levels of Atf1, a transcription factor
299 phosphorylated by Sty1 upon Sty1 activation (Shiozaki, Shiozaki and Russell, 1998;
300 Wilkinson *et al.*, 1996; Sun *et al.*, 2024). As expected, we find that Atf1 levels increase
301 upon cell exposure to 36°C or 42°C. (Fig. 4G, I), confirming that Sty1 is activated under
302 these experimental conditions.

303 Overall, these results indicate that Sty1 kinase activation during temperature stress
304 exerts a temperature specific effect on Orb6 kinase activity; Sty1 activation is necessary
305 to inhibit Orb6 activity and biological functions at 36°C while is not necessary at higher,
306 heat shock temperatures (42°C).

307

308 **Phosphorylation of the C-terminal hydrophobic motif Orb6-T456 is temperature**
309 **sensitive.**

310 To better study the molecular mechanisms of Orb6 kinase regulation, we
311 developed a phospho-specific antibody that recognizes Orb6 phosphorylation by an

312 upstream kinase at the C-terminal hydrophobic motif site, Threonine 456 (Fig. 5A).
313 Phosphorylation of the conserved phosphorylation site, Thr456, is essential for Orb6
314 function (Liu and Young, 2012). We validated the specificity of the phospho-Orb6-T456
315 antibody (hereafter referred to as pOrb6-T456) by performing a dot blot with 4 different
316 peptides of Orb6. The pOrb6-T456 antibody was specific only to phosphorylated
317 Threonine 456 and not to the corresponding unphosphorylated peptide or a similar
318 sequence at the C-terminal, Threonine 464 (Fig. 5B). Previous studies have identified
319 interactions between Nak1 kinase and Orb6 kinase suggesting that Nak1 functions
320 upstream of Orb6 (Liu and Young, 2012). However, direct phosphorylation of Orb6 by
321 Nak1 has yet to be reported. To test if Orb6-T456 phosphorylation is Nak1-dependent,
322 we exposed temperature-sensitive mutant of *nak1 (nak1-ts/orb3-167)* (Snell and Nurse,
323 1994; Leonhard and Nurse, 2005) to restrictive temperature (36°C) for 3 hours to
324 downregulate Nak1 activity and measured pOrb6-T456 levels in HA-tagged Orb6 (Fig.
325 5C). We find that pOrb6-T456 strongly decreases at 36°C in the *nak1-ts* mutant (Fig. 5C,
326 D). Further, we find that pOrb6-T456 also decreases to a lesser extent, at 36°C in the
327 control *nak1+* cells. (Fig. 5C, D). These results indicate the Orb6 phosphorylation at the
328 C-terminal hydrophobic motif T456 site is dependent on Nak1. Our observations also
329 suggest that Orb6-T456 phosphorylation is affected by heat stress.

330 To test if Sty1 kinase has a role in modulating Orb6-T456 phosphorylation, we
331 exposed cells to 36°C or 42°C for 30 minutes in the presence or absence of *sty1.* We
332 found that pOrb6-T456 phosphorylation decreases upon exposure to heat, in both control
333 *sty1*$^{+}$ or *sty1Δ* deletion mutants (Fig. 5E-F). However, loss of *sty1* leads to overall
334 increased levels of pOrb6-T456, as compared to control cells (Fig. 5E-F). This increase

335 is particularly evident at 25°C and 36°C, indicating that Sty1 regulates the levels of
336 phosphorylation of the Orb6 protein at the T456 site. Our observations suggest that the
337 increased levels of Orb6 phosphorylation, in the absence of Sty1, play a role in
338 maintaining sustained Orb6 kinase activity during heat stress at 36°C, thereby
339 suppressing the onset of Cdc42 exploratory dynamics and the induction of Sts5 granule
340 formation. This idea is supported by the observation that the extent of Gef1-S112
341 phosphorylation (a readout of Orb6 kinase activity) is similar in *sty1Δ* cells at 36°C and
342 unstressed wild-type controls at 25°C. Since Orb6 T456 phosphorylation decreases in
343 response to heat in both control and *sty1Δ* deletion mutant cells, our data also point to a
344 Sty1-independent mechanism of downregulation of Orb6 activity in response to
345 increasing heat stress.
346
347 **Discussion**
348
349 **Conserved NDR kinase Orb6 activity is thermo-sensitive.**
350 Proper cellular response to environmental fluctuations, such as heat exposure, is critical
351 for survival and is increasingly recognized as a key factor in human disease. Heat stress
352 disrupts essential cellular processes, including cell polarization (Vjestica *et al.*, 2013;
353 Pawlik *et al.*, 2013; Singh *et al.*, 2016; Delley and Hall, 1999) and protein translation
354 (Kedersha *et al.*, 2005; Grousl *et al.*, 2009). However, the underlying mechanisms
355 mediating these effects are not completely understood.
356 Here, we demonstrate that the conserved fission yeast NDR kinase Orb6,
357 homologous to mammalian STK38, is inactivated by heat stress, a process that alters the

358 pattern of active Cdc42 distribution at the membrane and facilitates stress granule
359 assembly. Overall, our findings provide experimental evidence explaining, at least in part,
360 some of the physiological effects of heat stress. We also uncover a regulatory mechanism
361 in which the stress-activated MAP kinase Sty1 negatively regulates Orb6 activity and
362 Orb6 C-terminal phosphorylation during heat stress (Fig. 6). This inhibition sensitizes cells
363 to temperature-specific heat stress, promoting adaptive metabolic responses and
364 thermotolerance. These findings underscore the pivotal role of NDR kinase signaling in
365 cellular adaptation to elevated temperatures. Further, our observations reveal a novel role
366 for conserved stress activated MAP kinase Sty1 in RNP granule formation, mediated by
367 Orb6 kinase.
368

369 **Orb6 downregulation fosters the emergence of exploratory Cdc42 dynamics during**
370 **heat stress.**

371 Cdc42 GTPase is a key regulator of cell polarization and is a highly conserved
372 Rho-family GTPase that regulates cell polarity, actin cytoskeleton organization, and
373 vesicle trafficking**.** In mammalian myoblasts, heat stress reduces cell migration, at least
374 in part through *CDC42* downregulation (Lu *et al.*, 2023). In fission yeast, under normal
375 conditions, active Cdc42-GTP oscillates between cell tips to promote polarized growth
376 (Das *et al.*, 2012). Upon environmental stress (including heat), Cdc42 adopts
377 an exploratory activation pattern along the cell membrane, deviating from its usual tip-
378 localized oscillations (Vjestica *et al.*, 2013; Chen *et al.*, 2019; Salat-Canela *et al.*, 2021;
379 Haupt, Ershov and Minc, 2018). Here, we show that during both mild and severe heat
380 stress, Orb6 kinase is inhibited. We previously showed that Orb6 inhibition leads to

381 dephosphorylation of Cdc42 regulators Gef1 and Rga3, and their release from the grip of
382 14-3-3- protein Rad24 (Das *et al.*, 2015; Doyle *et al.*, 2025), thereby switching on the
383 stress-activated Cdc42 module, which Gef1 and Rga3 are part of (Salat-Canela *et al.*,
384 2021; Doyle *et al.*, 2025). Our findings provide a mechanistic explanation of the process
385 of exploratory Cdc42 dynamics activation during heat stress. The functional role of
386 exploratory Cdc42 dynamics activation during heat stress, or other stresses, however, is
387 still unclear. Induction of exploratory Cdc42 dynamics during nitrogen deprivation (Chen
388 *et al.*, 2019) may have the function to facilitate the search for mating partners (Bendezú
389 and Martin, 2013). It is possible that the onset of Cdc42 exploratory dynamics in other
390 stresses is a byproduct of engaging the same MAP Kinase-Orb6 kinase regulatory axis
391 (Doyle *et al.*, 2025). Alternatively, temporary loss of cell polarity could signal a
392 physiological transition for the cell, providing the opportunity to activate and inactivate
393 alternative polarity sites upon recovery from stress. In fission yeast, recovery from a
394 disrupting event, such as actin depolymerization by Latrunculin A exposure, can alter the
395 pattern of Cdc42 distribution and ensuing cell polarity (Mutavchiev, Leda and Sawin,
396 2016). Finally, disrupting cell polarization, in combination with translational repression
397 (see below) may be part of a general physiological strategy to slow cell growth, in an effort
398 to preserve energy (Salat-Canela *et al.*, 2023) and extend cell lifespan (Chen *et al.*, 2019).
399

400 **Sts5 assembles into RNP granules and promotes thermotolerance.**

401 Upon exposure to a variety of external stressors, cells form stress granules that
402 help promote stress resilience and survival. The RNA binding protein Sts5 is highly
403 conserved in eukaryotes and is related to human Dis3L2, which is associated with

404 Perlman's syndrome and Wilm's tumor in humans. In fungi, Sts5 is closely related to
405 *Saccharomyces cerevisiae* and *Candida albicans* Ssd1, and *Neurospora crassa* GUL-1
406 (Astuti *et al.*, 2012; Lv *et al.*, 2015; Robinson *et al.*, 2015; Malecki *et al.*, 2013; Toda *et*
407 *al.*, 1996; Vaggi *et al.*, 2012; Jansen *et al.*, 2009; Kurischko *et al.*, 2011). These RNA-
408 binding regulators fine-tune translation of cell wall and morphogenesis-related genes,
409 crucial for stress adaptation, survival, and pathogenicity. In the yeasts
410 *Schizosaccharomyces pombe* and *Saccharomyces cerevisiae*, Sts5 and Ssd1,
411 respectively, bind to 5′ UTRs of mRNAs encoding cell wall proteins, repressing their
412 translation to control cell wall biogenesis (Nuñez *et al.*, 2016; Hogan *et al.*, 2008). Fission
413 yeast Sts5 also alters the translational landscape of mRNAs involved in polarized cell
414 growth and Cdc42 activity, regulating the Ras1-Scd1-Cdc42 regulatory axis (Chen *et al.*,
415 2019; Nuñez *et al.*, 2016). By promoting translational repression during nutritional stress,
416 both Sts5 and Ssd1 influence entry into and recovery from quiescence (Chen *et al.*, 2019;
417 Miles *et al.*, 2019). Finally, both Sts5 (this paper) and Ssd1 (Mir, Fiedler and Cashikar,
418 2009) are essential for tolerance to heat. Thus, the conservation of structure and cellular
419 function through such enormous evolutionary distance highlights the crucial role of these
420 RNA binding proteins in cell adaptation and survival.

421 How are these effects exerted in the cell? These proteins all share the property to
422 undergo liquid-liquid phase separation upon exposure to environmental stress, in a
423 manner that engages their N-terminal Intrinsically Disordered Domains (IDRs). The N-
424 terminal domain is crucial to mediate liquid-liquid phase separation of Sts5, Ssd1 and
425 GUL-1 into RNP granules, and is phosphorylated by conserved NDR kinase Orb6 in
426 *Schizosaccharomyces pombe* (Chen *et al.*, 2019), Cbk1 in *Saccharomyces cerevisia*e

427 (Kurischko *et al.*, 2011; Jansen *et al.*, 2009), and COT-1 in *Neurospora crassa* (Stein et
428 al., 2020) and other kinases (such as *S. pombe* Pak1 (Magliozzi and Moseley, 2021)).
429 We previously showed that serine 86 in the N terminus of Sts5 has a crucial role in
430 regulating Sts5 assembly into RNP granules, by mediating N-terminal Sts5 interaction
431 with 14-3-3 protein Rad24 (Chen *et al.*, 2019). Association of Sts5 with Rad24 inhibits
432 Sts5 phase separation into granules and maintains active protein translation of Sts5-
433 associated RNAs (Nuñez *et al.*, 2016). Conversely, mutation of serine 86 to alanine (*sts5-*
434 *S86A*), which prevents phosphorylation at that site, inhibits Rad24 association with Sts5
435 and thereby promotes RNP granule assembly and decreased translation of Sts5-
436 assicated RNAs (Chen *et al.*, 2019). We found that by subtly promoting RNP assembly,
437 the *sts5-S86A* mutation seemingly enhances cell resilience to stress exposure, extending
438 chronological lifespan during nutritional stress (Chen *et al.*, 2019). Here, we show that the
439 *sts5-S86A* mutation increases cellular resilience to heat stress, while loss of Sts5
440 increases heat stress vulnerability. We previously showed that Sts5 alters the
441 translational landscape of the cell by decreasing specific mRNA availability for translation,
442 such as *ssp1* mRNA and *efc25* mRNA ((Nuñez *et al.*, 2016); Fig. 2C). Consistent with a
443 role for Sts5 in translational repression during heat exposure, Ssp1 protein levels
444 drastically increase upon heat stress, when *sts5* is deleted (Nuñez *et al.*, 2016).

445 Processing bodies and stress granules are types of cytoplasmic ribonucleoprotein
446 (RNP) granules involved in mRNA regulation. A defining function of P-bodies and stress
447 granules is their dynamism, as these granules quickly assemble upon stress exposure
448 and disperse when stress conditions ameliorate. The difference between P-bodies
449 (processing bodies) and stress granules lies in their composition, formation triggers, and

450 cellular roles. P-bodies are involved in mRNA decay, storage, and translational repression
451 and contain enzymes for mRNA degradation (e.g., decapping enzymes Dcp1/Dcp2)
452 (Sakuno et al., 2004; Ingelfinger et al., 2002; van Dijk et al., 2002; Wang et al., 2002). P-
453 bodies are present under normal conditions but increase in size and number during
454 cellular stress. Stress granules, conversely, form in response to cellular stress (e.g., heat
455 shock, oxidative stress) and are triggered by translation initiation inhibition. Stress
456 granules store untranslated mRNAs to prevent their degradation and help cells recover
457 by allowing mRNAs to re-enter translation once stress resolves (Marcelo *et al.*, 2021;
458 Panas, Ivanov and Anderson, 2016).

459 While it is known that P-bodies and stress granules initially assemble through a
460 process known as liquid-liquid phase separation (Aguzzi and Altmeyer, 2016), much
461 remains to be elucidated regarding the mechanisms and factors involved in their
462 formation. Coalescence of RNA binding proteins into puncta is thought to promote
463 nucleation of both P-Bodies and stress granules (Kroschwald et al., 2015; Lin et al., 2015;
464 Elbaum-Garfinkle et al., 2015; Patel et al., 2015; Kato et al., 2012; Hyman, Weber and
465 Julicher, 2014; Brangwynne et al., 2009; Lee et al., 2013; Brangwynne, 2013; Becker and
466 Gitler, 2015).

467 During nitrogen or glucose deprivation, Sts5 proteins assemble into puncta that
468 partially co-localize with the P-Body marker Dcp1-mCherry (Chen *et al.*, 2019; Nuñez *et*
469 *al.*, 2016). In this paper, we find that also upon mild heat stress (36°C), Sts5 coalesces
470 into granules that colocalizes with P-body marker Dcp1. At the heat stress temperature
471 36°C, we do not observe formation of detectable Pabp1-containing stress granules. Upon
472 severe heat stress (42°C) when visible stress granules form, Sts5 also co-localize with

473 stress granules marker, Pabp1. Consistent with the fact that both P-Bodies and RNA
474 binding proteins are thought to promote the assembly of stress granules (Buchan,
475 Muhlrad and Parker, 2008; Wheeler et al., 2016), we find that loss of *sts5* strongly reduces
476 the number of stress granules and decreases cell survival during heat shock. Conversely,
477 Orb6 inhibition prior to heat exposure, which promotes Sts5 coalescence into granules,
478 (Nunez *et al.*, 2016; Chen *et al.*, 2019), substantially increases the amount of stress
479 granules formed in the cell during severe heat stress (42°C) and drastically increases
480 resilience to heat stress and heat shock. However, since increase in thermo-resilience is
481 much greater for Orb6 inhibition than for the s*ts5-S86A* mutation, it is likely that Orb6 has
482 additional roles in thermotolerance which are independent of Sts5.

483 Furthermore, since Orb6 kinase inhibition alone is not sufficient to drive stress
484 granule formation, it is likely that additional factors and regulatory controls play a role in
485 driving Sts5-mediated stress granule formation. For example, other factors such as the
486 vigilin homologue Vgl1 (Wen *et al.*, 2010), signaling factors such as calcineurin (Higa *et*
487 *al.*, 2015), and protein kinase C Pck2 (Kanda *et al.*, 2021) also associate with stress
488 granules in response to thermal stress, and stress granule formation is also stimulated in
489 response to heat stress by the RNA-binding protein Nrd1 (Satoh *et al.*, 2012).

490

491 **The MAP kinase Sty1-NDR kinase Orb6 regulatory axis regulates Cdc42 dynamics**
492 **and RNP granule assembly during heat stress.**

493 Conserved MAP kinase Sty1 is the stress-activated MAP kinase (SAPK) in fission
494 yeast. It is the central component of the Wis1–Sty1 MAPK pathway**,** analogous to
495 mammalian p38/JNK pathways. Heat stress transiently activates Sty1 through its dual

496 phosphorylation by Wis1 at two conserved residues, Threonine 171 and Tyrosine 173,
497 and leads to Sty1 nuclear accumulation (Degols, Shiozaki and Russell, 1996; Smith *et*
498 *al.*, 2002). Sty1 phosphorylation during heat stress is regulated by threonine and tyrosine
499 phosphatases, where tyrosine phosphatases, Pyp1 and Pyp2, are inhibited by heat
500 contributing to Sty1 activation and threonine phosphatases, Ptc1 and Ptc3, work to
501 attenuate Sty1 activity (Nguyen and Shiozaki, 1999). *Sty1Δ* mutants (Sty1 deletion) show
502 severe thermo-sensitivity**,** losing viability rapidly compared to wild type (Yamada *et al.*,
503 1997). Sty1 activation is essential for survival under both severe heat stress conditions
504 (≥42°C) (Berlanga *et al.*, 2010; Yamada *et al.*, 1997; Degols, Shiozaki and Russell, 1996),
505 as well as mild heat stress temperature 37°C (Yamada *et al.*, 1997)**.**

506 Our results indicate that Orb6 activity decreases upon exposure to heat stress and
507 heat shock. We recently reported that MAP kinase Sty1 negatively regulates Orb6 during
508 nitrogen starvation (Doyle *et al.*, 2025) providing a mechanistic understanding as to why
509 Sty1 activation elicits exploratory Cdc42 dynamics, a behavior that may facilitate ensuing
510 cell mating (Bendezú and Martin, 2013; Merlini *et al.*, 2016). We showed that Sty1 inhibits
511 Orb6 kinase, thereby releasing the Orb6 substrates Cdc42 GEF Gef1 and Cdc42 GAP
512 Rga3 from their association with 14-3-3- protein Rad24 (Doyle *et al.*, 2025), Sty1 also
513 directly phosphorylates Gef1 and Rga3, likely activating their enzymatic activity (Salat-
514 Canela *et al.*, 2021). This "coherent feedforward" mechanism promotes exploratory
515 Cdc42 dynamics during stress response (Salat-Canela *et al.*, 2021; Doyle *et al.*, 2025).

516 In this paper, we show that this Sty1-NDR kinase Orb6 regulatory axis has a
517 function in other stress responses, namely heat stress. Further, our data indicate that,
518 through Orb6, Sty1 also modulates the phase separation properties of mRNA binding

519 protein Sts5, and therefore the coalescence of P-bodies and stress granules in response
520 to heat exposure.

521 Interestingly, our observations show that loss of Sty1 completely suppresses the
522 effects of heat dependent Orb6 inhibition (the induction of Cdc42 exploratory dynamics,
523 Gef1 dephosphorylation, Sts5 aggregation) during moderate heat stress at 36 °C, but not
524 under heat shock conditions at 42°C. Experimentally, these findings suggest a
525 "temperature-specific" control of Orb6 kinase by Sty1 kinase, namely that the Sty1
526 function in Orb6 inhibition is only effective at sublethal 36 °C temperatures, but not at
527 42°C heat stress temperatures.

528

529 **The role of Orb6 T456 c-terminal hydrophobic motive in thermal sensation.**

530 To explore the mechanism behind this effect, we tested the role of the C-terminal
531 hydrophobic motif of Orb6 kinase in thermal sensation. The highly conserved hydrophobic
532 motif (HM) is a critical regulatory element in the AGC family of protein kinases**.** It contains
533 a phosphorylatable serine or threonine residue (in Orb6, Threonine 456) flanked by
534 hydrophobic amino acids. Phosphorylation of the HM is essential for stabilizing the active
535 conformation of the kinase, facilitating proper alignment of catalytic residues for efficient
536 substrate phosphorylation, and strongly correlates with kinase activity (Millward, Hess
537 and Hemmings, 1999; Hergovich *et al.*, 2006; Hergovich, 2013; Jansen *et al.*, 2006;
538 Brace, Hsu and Weiss, 2011; Parker *et al.*, 2020).

539 We discovered that the level of HM T456 phosphorylation in Orb6 kinase is
540 temperature-dependent, in a manner that is inversely correlated with increasing
541 temperatures. We find that upon loss of Sty1, the overall levels of Orb6-T456

542 phosphorylation substantially increase, an effect that is particularly striking at 25°C and
543 36°C, indicating that Sty1 has a role in the negative control of Orb6-T456 phosphorylation.
544 Further, we find that Orb6-T456 phosphorylation decreases during mild heat stress and
545 severe heat stress in both control or *sty1Δ* strains, suggesting that a Sty1-independent
546 mechanism also mediates Orb6 HM dephosphorylation during heat stress and heat
547 shock. The combined effect is that in *sty1Δ* cells exposed to heat stress at 36°C, the level
548 of Orb6 T456 phosphorylation is comparable to wild-type control cells grown in
549 unstressed conditions at 25°C. Consistent with the idea that the activity of Orb6 remains
550 high in *sty1Δ* cells at 36°C, Gef1 phosphorylation, Cdc42 distribution and Sts5 localization
551 are unperturbed, and cells appear unresponsive to heat stress. Overall, these results
552 indicate that Orb6 kinase inhibition by Sty1 kinase increases heat sensitivity during mild
553 heat stress (36°C), promoting assembly of Sts5 into granules (Fig.1E, 4A), coalescence
554 of Sts5 granules with P-bodies (Fig. S1), and downregulation of Sts5-associated mRNA
555 translation (Nuñez *et al.*, 2016). Thus, this finely tuned regulatory network ensures the
556 inhibition of Orb6 during mild heat stress (36°C), when stress granules do not form, but
557 when reprogramming of the translational landscape, and morphogenetic changes at the
558 membrane may be necessary for survival.

559 It is unclear what could be the Sty1-independent mechanism of temperature-
560 sensing that leads to Orb6 inactivation. One possible mechanism is that Nak1, the kinase
561 upstream of Orb6, is directly inhibited by heat stress. Another possible mechanism is that
562 heat affects protein structure of the Orb6 regulatory complex, perhaps the association of
563 the co-activator Mob2 to Orb6, or the interaction of the Mor2 scaffold with Nak1 and Orb6.
564 Direct inhibition of the Mob2-Orb6 complex by an inhibitory protein is also possible, as

565 detailed for the *S. cerevisiae* protein Lre1, which does not however have homologues in
566 *S. pombe* or higher eukaryotes (Mancini Lombardi *et al.*, 2013; Versele and Thevelein,
567 2001). Future experiments will address these possibilities.

568 In conclusion, our study highlights the role of the MAP kinase Sty1-NDR kinase
569 Orb6 regulatory axis in promoting thermotolerance during environmental heat exposure.
570 Thermotolerance refers to the ability of an organism, tissue, or cell to withstand elevated
571 temperatures without sustaining irreversible damage. The acquisition of thermotolerance
572 has enormous implications for the survival of crops, the spread of pathogenic organisms
573 to different latitudes, or the success of disease treatments, such as during cancer
574 hyperthermia therapy to enhance chemotherapy or radiation sensitivity. Thus, these
575 findings may have implications in higher eukaryotes due to the highly conserved nature
576 of NDR kinases across evolution.

577

578

579

580 **Materials and Methods:**

581 **Strains and Growth Medium**

582 *Schizosaccharomyces pombe* strains used in this study were derived from wild-type
583 strains 972 or 975 and are displayed in Table S1. *S. pombe* was maintained in yeast
584 extract plus supplements (YES) or Edinburgh minimal medium supplemented with 0.5%
585 ammonium chloride (EMMN) and additional supplements as needed (Histidine, Leucine,
586 Adenine, or Uracil) at a concentration of 225 mg/L. All strains were cultured at 25°C unless
587 otherwise noted. Liquid cultures were incubated at 180 RPM in a shaking incubator, and
588 all cultures were diluted daily such that they were maintained in logarithmic growth for a
589 minimum of 8 generations prior to performing experiments.

590 **Fluorescence Microscopy**

591 For experiments utilizing microscopy, samples were imaged with an Olympus BX61
592 fluorescent microscope using appropriate filters. Exposure times range from 1000-
593 2500ms for each experiment and remain consistent among all samples for that
594 experiment. Images were acquired and processed using Intelligent Imaging Innovations
595 SlideBook image analysis software (Version 6.0.4; Denver, CO) and prepared with Fiji
596 (Schindelin *et al.*, 2012).

597 **RNP Granule Induction**

598 To determine localization of Sts5 puncta relative to stress granules, we introduced the
599 marker Pabp1-DsRed, constructing a *sts5-3xGFP pabp1-DsRed* strain (FV2361). We
600 tested the localization of Sts5 relative to stress granules upon heat stress at 36°C or 42°C
601 for 30 minutes. To test the effects of glucose limitation, cells were grown in minimal
602 medium (EMM) containing 2% glucose for at least 8 generations, and then were

603 centrifuged, washed with the appropriate medium, and resuspended either in EMM
604 lacking glucose or in EMM with 2% glucose. Images are representative of samples from
605 three independent experiments.

606 **RNA Fluorescent In Situ Hybridization (RNA FISH)**

607 Localization of *ssp1* mRNA was determined using RNA-FISH as previously described,
608 with modifications according to Nunez *et al.* (Nunez *et al.*, 2016; Nilsson and
609 Sunnerhagen, 2011; Heinrich *et al.*, 2013; Brengues and Parker, 2007). *sts5-3xGFP*
610 *pabp1-DsRed* cells (FV2361) were cultured in EMM lacking glucose for 20 minutes prior
611 to fixation and hybridization of RNA was performed with 20-mer DNA oligonucleotides
612 (Stellaris) labeled with Quasar 705 fluorochromes.

613 **Glucose Starvation and Orb6 Inhibition Assays**

614 To determine if Sts5 was required for the formation of stress granules, a glucose
615 starvation assay was performed with *sts5*$^{+}$ *pabp1-DsRed* (FV1684) and *sts5Δ pabp1-*
616 *DsRed* (FV3192) mutants. Samples were cultured to log phase in minimal medium (EMM)
617 and were washed once with 5 mL minimal medium lacking glucose. Cells were then
618 resuspended in 5 mL minimal medium lacking glucose and were incubated at 25°C and
619 180 RPM in a shaking incubator for 20 minutes. Following incubation, 1 mL aliquots were
620 centrifuged at 4000 RPM for 1 minute and resuspended in a small amount of residual
621 medium. Microscopy was performed as previously described and the number of stress
622 granules was manually counted. This experiment was performed in triplicate, and n=90
623 cells per strain per strain per condition in total.

624 For Orb6 inhibition assays, *orb6-as2 pabp1-DsRed* (FV3226) and *pabp1-DsRed*
625 control (FV1684) strains were cultured to log phase in minimal medium containing

626 adenine. 1-NA-PP1 was added to samples at a final concentration of 50 μM. For assays
627 in which Orb6 was inhibited and then cells were heat shocked, 1-NA-PP1 was added to
628 cells 15 minutes prior to heat shock, whereas DMSO was added for control cells. Samples
629 were then shifted to a 42ºC shaking water bath incubator for 20 minutes. Additional
630 controls were maintained at 25 ºC. Microscopy was performed as previously described
631 and stress granules were manually counted. This experiment was performed in triplicate,
632 and n = 90 cells per strain per condition in total.

633 **Heat Shock Survival Assay**

634 *Wild-type* (FV2644), *sts5Δ* (FV2674), *sts5-HA* (FV2645), and *sts5-S86A-HA* (FV2649)
635 strains were cultured in EMM and maintained in log-phase for a minimum of eight
636 generations. Each strain was diluted to $O.D._{595nm} = 0.2$ (approximately $4x10^6$ cells/mL) in
637 5 mL EMM and allowed to grow at this density for one hour at 25°C shaking at 180 RPM.
638 Samples were either maintained at 25°C or heat shocked at 48°C for 15 minutes.
639 Following heat shock, experimental and control samples were each serially diluted, plated
640 in triplicate on EMM plates, and incubated at 25°C for approximately 72 hours. Colony
641 forming units per mL (CFU's/mL) were calculated for each condition, and percent survival
642 was calculated by dividing CFU's/mL for heat shocked replicates by their respective
643 untreated control CFU's/mL. Percent survival of each technical replicate was normalized
644 to the average untreated control percent survival. The average percent survival for each
645 strain is as follows: *wt*, 1.8%; *sts5Δ*, 0.2%; *sts5-HA*, 1.3%; and *sts5-S86A-HA*, 4.0%. This
646 experiment was performed in biological triplicate, and data was normalized to the average
647 wild-type percent survival for each independent experiment and subsequently graphed
648 as the relative survival rate. To determine the impact of intermediate to long-term

649 restrictive temperature on these strains, this experiment was repeated with modifications.
650 In this case, samples were incubated at 25°C or 36.5°C for 6 hours. Following incubation,
651 cells were serially diluted and plated in triplicate, and incubated at 25°C for approximately
652 72 hours. Calculation of CFU's/mL and normalization of data was performed as previously
653 described, and this experiment was performed in biological triplicate. The average
654 percent survival for each strain (normalized to the control at 25°C) is as follows: *wt*,
655 125.6%; *sts5Δ*, 65.2%; *sts5-HA*, 120.8%; and *sts5-S86A-HA*, 179.9%.

656 For heat shock survival analysis of the *orb6-as2* strain (FV2527) and its respective
657 wild-type control (FV2530), cells were initially pre-cultured in minimal medium
658 supplemented with adenine at 180 RPM and 32ºC. In order to repress the expression of
659 *orb6-as2* the culture was split into two sets, either with or without thiamine at a final
660 concentration of 15 μM and was allowed to grow for ~16 hours. Cells were diluted to an
661 equivalent $O.D._{595nm}$ of 0.2 ($4x10^6$ cells/mL) in appropriate media, and cells were allowed
662 to grow for an additional 2 hours. Samples were then heat shocked in a 48ºC shaking
663 water bath for 15 minutes while controls were maintained at 32ºC. All samples were then
664 serially diluted and plated on minimal medium supplemented with adenine, but lacking
665 thiamine, for subsequent quantification of CFU's/mL as previously described. The
666 average percent survival for each strain is as follows: *wt* -Thiamine, 0.1%; *wt* +Thiamine,
667 0.1%; *orb6-as2* -Thiamine, 0.1%; and *orb6-as2* +Thiamine, 18.9%.

668 **Temperature Dependent Analysis of Sts5 Puncta**

669 *sts5-3xYFP* (FV2518) and *sts5-S86A-3xYFP* (FV2522) strains were used to determine
670 whether Sts5 puncta are induced at lower temperatures when Sts5 is hyperactive as
671 compared to a wild-type allele. Each strain was cultured to log-phase in EMM, diluted to

672 $O.D._{595nm}$= 0.1, and cells were allowed to grow for a minimum of 1 hour at 25°C. Aliquots
673 of each strain were created, and samples were heat shocked at 29°C, 32°C, 35.5°C, or
674 42°C for 30 minutes. Control cells were maintained at 25°C throughout the experiment.
675 Following exposure to heat shock, samples were imaged using an Olympus BX61
676 microscope. To determine differences in number of puncta, 20 cells per strain were
677 manually scored for Sts5 (YFP) puncta at each temperature.

678 **Development of anti-pOrb6-T456 phospho-specific antibody**

679 The anti-pOrb6-T456 phospho-specific antibody was custom-made by 21st Century
680 Biochemicals against a synthetic peptide corresponding to the phosphorylated Thr-456
681 (amino acids 449-462, NLAFLGYT*YKKFNY) of the fission yeast Orb6 protein. To detect
682 pOrb6-T456, we used a strain expressing N-terminally tagged HA-Orb6 *(HA-orb6-as2)*,
683 integrated in single copy behind the *nmt1* promoter, since increased expression of Orb6
684 allows for better detection of pOrb6-T456, as compared to C-terminally tagged Orb6-HA
685 or endogenous Orb6 where the detection signal is too low.

686 **Protein extraction and western blot analysis**

687 Protein extraction was modified from previously described protocol(Matsuo *et al.*,
688 2006) and performed as previously described (Doyle *et al.*, 2025). ~7.5×10^7 total cells
689 growing exponentially were harvested and cell pellets were resuspended in 300µL of H_2O
690 with protease and phosphatase inhibitor cocktail (Halt™ Protease and Phosphatase
691 Inhibitor Cocktail (100X)) and transferred to 1.5mL microcentrifuge tube. 300µL of 0.6M
692 NaOH with inhibitor cocktail (see above) was added to the cells and resuspended. Cells
693 were left to incubate for 5 minutes at room temperature, inverting the tubes 2-3 times
694 halfway through incubation. Cells were then centrifuged at 2300 RCF for 2 minutes. The
695 supernatant was discarded, and the pellet was resuspended in 75µL modified SDS buffer

696 (60mM Tris-HCl [pH 6.8], 4% 2-Mercaptoethanol, 4% SDS, 5% glycerol) with inhibitor
697 cocktail (see above) and boiled at 98°C for 3 minutes. Cells were placed on ice and
698 centrifuged at 4°C at 3500 RCF for 1 minute. 65μL of the supernatant (protein extract)
699 was collected with 60μL stored at -80°C immediately, and 5μL used for downstream
700 protein quantification assay. To quantify protein, the RC DC protein assay kit was used
701 as it is compatible with the concentration of reducing agents and detergents present in
702 the modified SDS buffer.

703 Standard western blotting procedures were performed as follows: protein was
704 separated using SDS-PAGE and transferred onto a nitrocellulose membrane. The
705 membranes were probed with antibodies of interest and visualized through fluorescent
706 detection on Li-Cor Odyssey CLx. Gef1-3YFP strains were used in detecting total Gef1
707 protein with anti-GFP (Roche, CAT#: 11814460001; RRID:AB_390913; dilution factor
708 (DF): 1:1000) and phosphorylated Gef1-S112 was detected using a custom-made
709 previously described antibody(Chen *et al.*, 2019). HA-Orb6as2 strains were used in
710 detecting total Orb6 protein with anti-HA (Biolegend, CAT#901501; RRID:AB_2565006;
711 DF: 1:3000) and phosphorylated Orb6-T456 was detected using a custom-made antibody
712 (see subsection “Development of anti-pOrb6-T456 phosphospecific antibody” in Methods
713 section). Anti-β-Actin (Abcam, CAT#: AB8224; RRID:AB_449644; DF: 1:4000) was used
714 as a loading control for all experiments. Two-color detection was used with using LiCor
715 IRDye secondary antibodies anti-rabbit 800CW (Li-Cor, CAT#: 926-32211;
716 RRID:AB_621843; DF: 1:15000) for anti-pGef1-S112 or anti-pOrb6-T456 and anti-mouse
717 680RD (Li-Cor, CAT#: 102673-408; RRID:AB_10956588; DF: 1:15000) for anti-GFP
718 (Gef1-3YFP) or anti-HA (HA-Orb6as2). Quantification of the blots was performed using

719 Image Studio software. To quantify, a rectangle was drawn around the signal band of
720 interest and pixel intensity was recorded. To remove background signal, background
721 settings were set to median, segment: top and bottom, border width: 3. With the pixel
722 intensity measurements, a ratio was determined between pGef1-S112 or pOrb6-T456
723 (fluorescent channel 800) and total Gef1-3YFP or total HA-Orb6as2 (fluorescent channel
724 700) to measure how much total Gef1-3YFP protein is phosphorylated at S112 or total
725 HA-Orb6as2 protein is phosphorylated at T456. Data was normalized by creating a ratio
726 with all values with the average ratio of control strains and/or conditions. Similar
727 quantification was performed to measure ratio of Atf1 to β-Actin during heat stress in
728 control cells and *sty1* deletion mutants using anti-Atf1 (Abcam, CAT#: AB18123;
729 RRID:AB_444264; DF: 1:2000) and anti-β-Actin (Abcam).
730
731 **Quantification and statistical analysis**
732 Data are presented as described in legends. Experiments were completed in
733 independent biological triplicates. A two-tailed unpaired Student's t test was used to
734 assess statistical significance between two groups. One-way or two-way analysis of
735 variance (ANOVA) followed by appropriate post hoc test was applied to evaluate the
736 difference between more than two groups (one-way) or more than 2 groups and more
737 than one condition (two-way). Statistical analyses and visualization were performed with
738 GraphPad Prism 10 (GraphPad Software, San Diego, CA). p-value < 0.05 was set as
739 the threshold for statistical significance. Power analyses were performed using G*Power
740 to determine minimum sample size(Faul *et al.*, 2007; Kang, 2021).
741

742 **Competing Interests**

743 The authors declare no competing interests.

744

745 **Funding**

746 Research reported in this publication was supported by the National Institute of Health

747 (NIH) R01 GM129514 and by the Sylvester Comprehensive Cancer Center which

748 receives funding from the National Cancer Institute of the National Institutes of Health

749 under Award Number P30CA240139.

750

751 **Data and Resource Availability**

752 Data and resource availability: All relevant data and details of resources can be found

753 within the article and its supplementary information.

754
755
756
757
758

759 **References**
760

761 1. Adeyinka, A., Emberley, E., Niu, Y., Snell, L., Murphy, L. C., Sowter, H., Wykoff, C. C., Harris,
762 A. L. and Watson, P. H. (2002) 'Analysis of gene expression in ductal carcinoma in situ
763 of the breast', *Clin Cancer Res,* 8(12), pp. 3788-95.
764 2. Aguzzi, A. and Altmeyer, M. (2016) 'Phase Separation: Linking Cellular Compartmentalization
765 to Disease', *Trends Cell Biol,* 26(7), pp. 547-558.
766 3. Alberti, S. and Dormann, D. (2019) 'Liquid-Liquid Phase Separation in Disease', *Annu Rev*
767 *Genet,* 53, pp. 171-194.
768 4. Anderson, P., Kedersha, N. and Ivanov, P. (2015) 'Stress granules, P-bodies and cancer',
769 *Biochim Biophys Acta,* 1849(7), pp. 861-70.
770 5. Astuti, D., Morris, M. R., Cooper, W. N., Staals, R. H., Wake, N. C., Fews, G. A., Gill, H.,
771 Gentle, D., Shuib, S., Ricketts, C. J., Cole, T., van Essen, A. J., van Lingen, R. A., Neri,
772 G., Opitz, J. M., Rump, P., Stolte-Dijkstra, I., Muller, F., Pruijn, G. J., Latif, F. and Maher,
773 E. R. (2012) 'Germline mutations in DIS3L2 cause the Perlman syndrome of overgrowth
774 and Wilms tumor susceptibility', *Nat Genet,* 44(3), pp. 277-84.
775 6. Becker, L. A. and Gitler, A. D. (2015) 'It's all starting to come together', *Elife,* 4.
776 7. Bendezú, Felipe O. and Martin, Sophie G. (2013) 'Cdc42 Explores the Cell Periphery for
777 Mate Selection in Fission Yeast', *Current Biology,* 23(1), pp. 42-47.
778 8. Berlanga, J. J., Rivero, D., Martín, R., Herrero, S., Moreno, S. and de Haro, C. (2010) 'Role of
779 mitogen-activated protein kinase Sty1 in regulation of eukaryotic initiation factor 2alpha
780 kinases in response to environmental stress in Schizosaccharomyces pombe', *Eukaryot*
781 *Cell,* 9(1), pp. 194-207.
782 9. Brace, J., Hsu, J. and Weiss, E. L. (2011) 'Mitotic exit control of the Saccharomyces
783 cerevisiae Ndr/LATS kinase Cbk1 regulates daughter cell separation after cytokinesis',
784 *Mol Cell Biol,* 31(4), pp. 721-35.
785 10. Brangwynne, C. P. (2013) 'Phase transitions and size scaling of membrane-less organelles',
786 *J Cell Biol,* 203(6), pp. 875-81.
787 11. Brangwynne, C. P., Eckmann, C. R., Courson, D. S., Rybarska, A., Hoege, C., Gharakhani,
788 J., Julicher, F. and Hyman, A. A. (2009) 'Germline P granules are liquid droplets that
789 localize by controlled dissolution/condensation', *Science,* 324(5935), pp. 1729-32.
790 12. Brengues, M. and Parker, R. (2007) 'Accumulation of polyadenylated mRNA, Pab1p, eIF4E,
791 and eIF4G with P-bodies in Saccharomyces cerevisiae', *Mol Biol Cell,* 18(7), pp. 2592-
792 602.

793 13. Buchan, J. R., Muhlrad, D. and Parker, R. (2008) 'P bodies promote stress granule
794 assembly in Saccharomyces cerevisiae', *J Cell Biol,* 183(3), pp. 441-55.
795 14. Chen, C., Pino, M. R., Haller, P. R. and Verde, F. (2019) 'Conserved NDR/LATS kinase
796 controls RAS GTPase activity to regulate cell growth and chronological lifespan',
797 *Molecular Biology of the Cell,* 30(20), pp. 2598-2616.
798 15. Chiba, S., Ikeda, M., Katsunuma, K., Ohashi, K. and Mizuno, K. (2009) 'MST2- and Furry-
799 mediated activation of NDR1 kinase is critical for precise alignment of mitotic
800 chromosomes', *Curr Biol,* 19(8), pp. 675-81.
801 16. Ciocca, D. R., Arrigo, A. P. and Calderwood, S. K. (2013) 'Heat shock proteins and heat
802 shock factor 1 in carcinogenesis and tumor development: an update', *Arch Toxicol,*
803 87(1), pp. 19-48.
804 17. Coll, P. M., Trillo, Y., Ametzazurra, A. and Perez, P. (2003) 'Gef1p, a new guanine
805 nucleotide exchange factor for Cdc42p, regulates polarity in Schizosaccharomyces
806 pombe', *Mol Biol Cell,* 14(1), pp. 313-23.
807 18. Cornils, H., Kohler, R. S., Hergovich, A. and Hemmings, B. A. (2011) 'Downstream of human
808 NDR kinases: impacting on c-myc and p21 protein stability to control cell cycle
809 progression', *Cell Cycle,* 10(12), pp. 1897-904.
810 19. Cornils, H., Stegert, M. R., Hergovich, A., Hynx, D., Schmitz, D., Dirnhofer, S. and
811 Hemmings, B. A. (2010) 'Ablation of the kinase NDR1 predisposes mice to the
812 development of T cell lymphoma', *Sci Signal,* 3(126), pp. ra47.
813 20. Das, M., Drake, T., Wiley, D. J., Buchwald, P., Vavylonis, D. and Verde, F. (2012)
814 'Oscillatory Dynamics of Cdc42 GTPase in the Control of Polarized Growth', *Science,*
815 337(6091), pp. 239-243.
816 21. Das, M., Nuñez, I., Rodriguez, M., Wiley, D. J., Rodriguez, J., Sarkeshik, A., R.III, Y. J.,
817 Buchwald, P. and Verde, F. (2015) 'Phosphorylation-dependent inhibition of Cdc42 GEF
818 Gef1 by 14-3-3 protein Rad24 spatially regulates Cdc42 GTPase activity and oscillatory
819 dynamics during cell morphogenesis', *Molecular Biology of the Cell,* 26(19), pp. 3520-
820 3534.
821 22. Das, M., Wiley, D. J., Chen, X., Shah, K. and Verde, F. (2009) 'The conserved NDR kinase
822 Orb6 controls polarized cell growth by spatial regulation of the small GTPase Cdc42',
823 *Curr Biol,* 19(15), pp. 1314-9.
824 23. Degols, G., Shiozaki, K. and Russell, P. (1996) 'Activation and regulation of the Spc1 stress-
825 activated protein kinase in Schizosaccharomyces pombe', *Mol Cell Biol,* 16(6), pp. 2870-
826 7.

24. Delley, P. A. and Hall, M. N. (1999) 'Cell wall stress depolarizes cell growth via hyperactivation of RHO1', *J Cell Biol,* 147(1), pp. 163-74.
25. Desai, M., Gulati, K., Agrawal, M., Ghumra, S. and Sahoo, P. K. (2026) 'Stress granules: Guardians of cellular health and triggers of disease', *Neural Regen Res,* 21(2), pp. 588-597.
26. Ding, X. and Gao, B. (2025) 'Heat Stress-Mediated Multi-Organ Injury: Pathophysiology and Treatment Strategies', *Comprehensive Physiology,* 15(3), pp. e70012.
27. Doyle, L. P., Chen, J.-S., Gould, K. L., McCollum, D. and Verde, F. (2025) 'Control of stress-activated Cdc42 dynamics by the MAP kinase Sty1—NDR kinase Orb6 regulatory axis', *iScience,* 28(9).
28. Dressler, C., Minet, O., Beuthan, J., Novkov, V. and Müller, G. (2005) 'Microscopical heat stress investigations under application of quantum dots', *J Biomed Opt,* 10(4), pp. 41209.
29. Elbaum-Garfinkle, S., Kim, Y., Szczepaniak, K., Chen, C. C., Eckmann, C. R., Myong, S. and Brangwynne, C. P. (2015) 'The disordered P granule protein LAF-1 drives phase separation into droplets with tunable viscosity and dynamics', *Proc Natl Acad Sci U S A,* 112(23), pp. 7189-94.
30. Faul, F., Erdfelder, E., Lang, A. G. and Buchner, A. (2007) 'G*Power 3: a flexible statistical power analysis program for the social, behavioral, and biomedical sciences', *Behav Res Methods,* 39(2), pp. 175-91.
31. Fouani, M., Basset, C. A., Mangano, G. D., Leone, L. G., Lawand, N. B., Leone, A. and Barone, R. (2022) 'Heat Shock Proteins Alterations in Rheumatoid Arthritis', *Int J Mol Sci,* 23(5).
32. Gallo Castro, D. and Martin, S. G. (2018) 'Differential GAP requirement for Cdc42-GTP polarization during proliferation and sexual reproduction', *Journal of Cell Biology,* 217(12), pp. 4215-4229.
33. Gilks, N., Kedersha, N., Ayodele, M., Shen, L., Stoecklin, G., Dember, L. M. and Anderson, P. (2004) 'Stress granule assembly is mediated by prion-like aggregation of TIA-1', *Mol Biol Cell,* 15(12), pp. 5383-98.
34. Gomez-Pastor, R., Burchfiel, E. T. and Thiele, D. J. (2018) 'Regulation of heat shock transcription factors and their roles in physiology and disease', *Nat Rev Mol Cell Biol,* 19(1), pp. 4-19.
35. Grousl, T., Ivanov, P., Frýdlová, I., Vasicová, P., Janda, F., Vojtová, J., Malínská, K., Malcová, I., Nováková, L., Janosková, D., Valásek, L. and Hasek, J. (2009) 'Robust heat

861 shock induces eIF2alpha-phosphorylation-independent assembly of stress granules
862 containing eIF3 and 40S ribosomal subunits in budding yeast, Saccharomyces
863 cerevisiae', *J Cell Sci,* 122(Pt 12), pp. 2078-88.
864 36. Gungor, B., Gombos, I., Crul, T., Ayaydin, F., Szabó, L., Török, Z., Mátés, L., Vígh, L. and
865 Horváth, I. (2014) 'Rac1 Participates in Thermally Induced Alterations of the
866 Cytoskeleton, Cell Morphology and Lipid Rafts, and Regulates the Expression of Heat
867 Shock Proteins in B16F10 Melanoma Cells', *PLOS ONE,* 9(2), pp. e89136.
868 37. Guzikowski, A. R., Chen, Y. S. and Zid, B. M. (2019) 'Stress-induced mRNP granules: Form
869 and function of processing bodies and stress granules', *Wiley Interdiscip Rev RNA,*
870 10(3), pp. e1524.
871 38. Hanyu, Y., Imai, K. K., Kawasaki, Y., Nakamura, T., Nakaseko, Y., Nagao, K., Kokubu, A.,
872 Ebe, M., Fujisawa, A., Hayashi, T., Obuse, C. and Yanagida, M. (2009)
873 'Schizosaccharomyces pombe cell division cycle under limited glucose requires Ssp1
874 kinase, the putative CaMKK, and Sds23, a PP2A-related phosphatase inhibitor', *Genes*
875 *Cells,* 14(5), pp. 539-54.
876 39. Haupt, A., Ershov, D. and Minc, N. (2018) 'A Positive Feedback between Growth and
877 Polarity Provides Directional Persistency and Flexibility to the Process of Tip Growth',
878 *Current Biology,* 28(20), pp. 3342-3351.e3.
879 40. Hauschild, A., Engel, G., Brenner, W., Glaser, R., Monig, H., Henze, E. and Christophers, E.
880 (1999) 'S100B protein detection in serum is a significant prognostic factor in metastatic
881 melanoma', *Oncology,* 56(4), pp. 338-44.
882 41. Heinrich, S., Geissen, E. M., Kamenz, J., Trautmann, S., Widmer, C., Drewe, P., Knop, M.,
883 Radde, N., Hasenauer, J. and Hauf, S. (2013) 'Determinants of robustness in spindle
884 assembly checkpoint signalling', *Nat Cell Biol,* 15(11), pp. 1328-39.
885 42. Hergovich, A. (2013) 'Regulation and functions of mammalian LATS/NDR kinases: looking
886 beyond canonical Hippo signalling', *Cell & Bioscience,* 3(1), pp. 32.
887 43. Hergovich, A., Kohler, R. S., Schmitz, D., Vichalkovski, A., Cornils, H. and Hemmings, B. A.
888 (2009) 'The MST1 and hMOB1 tumor suppressors control human centrosome
889 duplication by regulating NDR kinase phosphorylation', *Curr Biol,* 19(20), pp. 1692-702.
890 44. Hergovich, A., Lamla, S., Nigg, E. A. and Hemmings, B. A. (2007) 'Centrosome-associated
891 NDR kinase regulates centrosome duplication', *Mol Cell,* 25(4), pp. 625-34.
892 45. Hergovich, A., Stegert, M. R., Schmitz, D. and Hemmings, B. A. (2006) 'NDR kinases
893 regulate essential cell processes from yeast to humans', *Nature Reviews Molecular Cell*
894 *Biology,* 7(4), pp. 253-264.

895 46. Higa, M., Kita, A., Hagihara, K., Kitai, Y., Doi, A., Nagasoko, R., Satoh, R. and Sugiura, R.
896 (2015) 'Spatial control of calcineurin in response to heat shock in fission yeast', *Genes*
897 *Cells,* 20(2), pp. 95-107.
898 47. Hogan, D. J., Riordan, D. P., Gerber, A. P., Herschlag, D. and Brown, P. O. (2008) 'Diverse
899 RNA-binding proteins interact with functionally related sets of RNAs, suggesting an
900 extensive regulatory system', *PLoS Biol,* 6(10), pp. e255.
901 48. Hu, C., Yang, J., Qi, Z., Wu, H., Wang, B., Zou, F., Mei, H., Liu, J., Wang, W. and Liu, Q.
902 (2022) 'Heat shock proteins: Biological functions, pathological roles, and therapeutic
903 opportunities', *MedComm (2020),* 3(3), pp. e161.
904 49. Hyman, A. A., Weber, C. A. and Julicher, F. (2014) 'Liquid-liquid phase separation in
905 biology', *Annu Rev Cell Dev Biol,* 30, pp. 39-58.
906 50. Ingelfinger, D., Arndt-Jovin, D. J., Luhrmann, R. and Achsel, T. (2002) 'The human LSm1-7
907 proteins colocalize with the mRNA-degrading enzymes Dcp1/2 and Xrnl in distinct
908 cytoplasmic foci', *Rna,* 8(12), pp. 1489-501.
909 51. Jansen, J. M., Barry, M. F., Yoo, C. K. and Weiss, E. L. (2006) 'Phosphoregulation of Cbk1
910 is critical for RAM network control of transcription and morphogenesis', *J Cell Biol,*
911 175(5), pp. 755-66.
912 52. Jansen, J. M., Wanless, A. G., Seidel, C. W. and Weiss, E. L. (2009) 'Cbk1 regulation of the
913 RNA-binding protein Ssd1 integrates cell fate with translational control', *Curr Biol,*
914 19(24), pp. 2114-20.
915 53. Jung, M. K., Kim, K. Y., Lee, N. Y., Kang, Y. S., Hwang, Y. J., Kim, Y., Sung, J. J., McKee,
916 A., Kowall, N., Lee, J. and Ryu, H. (2013) 'Expression of taurine transporter (TauT) is
917 modulated by heat shock factor 1 (HSF1) in motor neurons of ALS', *Mol Neurobiol,*
918 47(2), pp. 699-710.
919 54. Kanda, Y., Satoh, R., Takasaki, T., Tomimoto, N., Tsuchiya, K., Tsai, C. A., Tanaka, T.,
920 Kyomoto, S., Hamada, K., Fujiwara, T. and Sugiura, R. (2021) 'Sequestration of the PKC
921 ortholog Pck2 in stress granules as a feedback mechanism of MAPK signaling in fission
922 yeast', *J Cell Sci,* 134(2).
923 55. Kang, H. (2021) 'Sample size determination and power analysis using the G*Power
924 software', *J Educ Eval Health Prof,* 18, pp. 17.
925 56. Kato, M., Han, T. W., Xie, S., Shi, K., Du, X., Wu, L. C., Mirzaei, H., Goldsmith, E. J.,
926 Longgood, J., Pei, J., Grishin, N. V., Frantz, D. E., Schneider, J. W., Chen, S., Li, L.,
927 Sawaya, M. R., Eisenberg, D., Tycko, R. and McKnight, S. L. (2012) 'Cell-free formation

928 of RNA granules: low complexity sequence domains form dynamic fibers within
929 hydrogels', *Cell,* 149(4), pp. 753-67.
930 57. Kedersha, N., Stoecklin, G., Ayodele, M., Yacono, P., Lykke-Andersen, J., Fritzler, M. J.,
931 Scheuner, D., Kaufman, R. J., Golan, D. E. and Anderson, P. (2005) 'Stress granules
932 and processing bodies are dynamically linked sites of mRNP remodeling', *J Cell Biol,*
933 169(6), pp. 871-84.
934 58. Kroschwald, S. and Alberti, S. (2017) 'Gel or Die: Phase Separation as a Survival Strategy',
935 *Cell,* 168(6), pp. 947-948.
936 59. Kroschwald, S., Maharana, S., Mateju, D., Malinovska, L., Nuske, E., Poser, I., Richter, D.
937 and Alberti, S. (2015) 'Promiscuous interactions and protein disaggregases determine
938 the material state of stress-inducible RNP granules', *Elife,* 4, pp. e06807.
939 60. Kurischko, C., Kim, H. K., Kuravi, V. K., Pratzka, J. and Luca, F. C. (2011) 'The yeast Cbk1
940 kinase regulates mRNA localization via the mRNA-binding protein Ssd1', *J Cell Biol,*
941 192(4), pp. 583-98.
942 61. Lee, C. F., Brangwynne, C. P., Gharakhani, J., Hyman, A. A. and Julicher, F. (2013) 'Spatial
943 organization of the cell cytoplasm by position-dependent phase separation', *Phys Rev*
944 *Lett,* 111(8), pp. 088101.
945 62. Leonhard, K. and Nurse, P. (2005) 'Ste20/GCK kinase Nak1/Orb3 polarizes the actin
946 cytoskeleton in fission yeast during the cell cycle', *Journal of Cell Science,* 118(5), pp.
947 1033-1044.
948 63. Lin, Y., Protter, D. S., Rosen, M. K. and Parker, R. (2015) 'Formation and Maturation of
949 Phase-Separated Liquid Droplets by RNA-Binding Proteins', *Mol Cell,* 60(2), pp. 208-19.
950 64. Liu, G. and Young, D. (2012) 'Conserved Orb6 Phosphorylation Sites Are Essential for
951 Polarized Cell Growth in Schizosaccharomyces pombe', *PLOS ONE,* 7(5), pp. e37221.
952 65. Lu, J., Li, H., Yu, D., Zhao, P. and Liu, Y. (2023) 'Heat stress inhibits the proliferation and
953 differentiation of myoblasts and is associated with damage to mitochondria', *Front Cell*
954 *Dev Biol,* 11, pp. 1171506.
955 66. Lv, H., Zhu, Y., Qiu, Y., Niu, L., Teng, M. and Li, X. (2015) 'Structural analysis of Dis3l2, an
956 exosome-independent exonuclease from Schizosaccharomyces pombe', *Acta*
957 *Crystallogr D Biol Crystallogr,* 71(Pt 6), pp. 1284-94.
958 67. Magliozzi, J. O. and Moseley, J. B. (2021) 'Pak1 kinase controls cell shape through
959 ribonucleoprotein granules', *Elife,* 10.
960 68. Mahboubi, H. and Stochaj, U. (2017) 'Cytoplasmic stress granules: Dynamic modulators of
961 cell signaling and disease', *Biochim Biophys Acta Mol Basis Dis,* 1863(4), pp. 884-895.

962 69. Malecki, M., Viegas, S. C., Carneiro, T., Golik, P., Dressaire, C., Ferreira, M. G. and
963 Arraiano, C. M. (2013) 'The exoribonuclease Dis3L2 defines a novel eukaryotic RNA
964 degradation pathway', *EMBO J,* 32(13), pp. 1842-54.
965 70. Mancini Lombardi, I., Palani, S., Meitinger, F., Darieva, Z., Hofmann, A., Sharrocks, A. D.
966 and Pereira, G. (2013) 'Lre1 directly inhibits the NDR/Lats kinase Cbk1 at the cell
967 division site in a phosphorylation-dependent manner', *Curr Biol,* 23(18), pp. 1736-45.
968 71. Marcelo, A., Koppenol, R., de Almeida, L. P., Matos, C. A. and Nóbrega, C. (2021) 'Stress
969 granules, RNA-binding proteins and polyglutamine diseases: too much aggregation?',
970 *Cell Death & Disease,* 12(6), pp. 592.
971 72. Matsuo, Y., Asakawa, K., Toda, T. and Katayama, S. (2006) 'A Rapid Method for Protein
972 Extraction from Fission Yeast', *Bioscience, Biotechnology, and Biochemistry,* 70(8), pp.
973 1992-1994.
974 73. Matsusaka, T., Hirata, D., Yanagida, M. and Toda, T. (1995) 'A novel protein kinase gene
975 ssp1+ is required for alteration of growth polarity and actin localization in fission yeast',
976 *EMBO J,* 14(14), pp. 3325-38.
977 74. Merlini, L., Khalili, B., Bendezú, F. O., Hurwitz, D., Vincenzetti, V., Vavylonis, D. and Martin,
978 S. G. (2016) 'Local Pheromone Release from Dynamic Polarity Sites Underlies Cell-Cell
979 Pairing during Yeast Mating', *Curr Biol,* 26(8), pp. 1117-25.
980 75. Miles, S., Li, L. H., Melville, Z. and Breeden, L. L. (2019) 'Ssd1 and the cell wall integrity
981 pathway promote entry, maintenance, and recovery from quiescence in budding yeast',
982 *Mol Biol Cell,* 30(17), pp. 2205-2217.
983 76. Millar, J. B., Buck, V. and Wilkinson, M. G. (1995) 'Pyp1 and Pyp2 PTPases
984 dephosphorylate an osmosensing MAP kinase controlling cell size at division in fission
985 yeast', *Genes Dev,* 9(17), pp. 2117-30.
986 77. Millward, T. A., Heizmann, C. W., Schafer, B. W. and Hemmings, B. A. (1998) 'Calcium
987 regulation of Ndr protein kinase mediated by S100 calcium-binding proteins', *Embo j,*
988 17(20), pp. 5913-22.
989 78. Millward, T. A., Hess, D. and Hemmings, B. A. (1999) 'Ndr Protein Kinase Is Regulated by
990 Phosphorylation on Two Conserved Sequence Motifs *', *Journal of Biological Chemistry,*
991 274(48), pp. 33847-33850.
992 79. Mir, S. S., Fiedler, D. and Cashikar, A. G. (2009) 'Ssd1 is required for thermotolerance and
993 Hsp104-mediated protein disaggregation in Saccharomyces cerevisiae', *Mol Cell Biol,*
994 29(1), pp. 187-200.

995 80. Mutavchiev, Delyan R., Leda, M. and Sawin, Kenneth E. (2016) 'Remodeling of the Fission
996 Yeast Cdc42 Cell-Polarity Module via the Sty1 p38 Stress-Activated Protein Kinase
997 Pathway', *Current Biology,* 26(21), pp. 2921-2928.
998 81. Napoletano, F., Occhi, S., Calamita, P., Volpi, V., Blanc, E., Charroux, B., Royet, J. and
999 Fanto, M. (2011) 'Polyglutamine Atrophin provokes neurodegeneration in Drosophila by
1000 repressing fat', *Embo j,* 30(5), pp. 945-58.
1001 82. Nguyen, A. N. and Shiozaki, K. (1999) 'Heat-shock-induced activation of stress MAP kinase
1002 is regulated by threonine- and tyrosine-specific phosphatases', *Genes Dev,* 13(13), pp.
1003 1653-63.
1004 83. Nilsson, D. and Sunnerhagen, P. (2011) 'Cellular stress induces cytoplasmic RNA granules
1005 in fission yeast', *RNA,* 17(1), pp. 120-33.
1006 84. Nunez, I., Rodriguez Pino, M., Wiley, D. J., Das, M. E., Chen, C., Goshima, T., Kume, K.,
1007 Hirata, D., Toda, T. and Verde, F. (2016) 'Spatial control of translation repression and
1008 polarized growth by conserved NDR kinase Orb6 and RNA-binding protein Sts5', *Elife,* 5.
1009 85. Nuñez, I., Rodriguez Pino, M., Wiley, D. J., Das, M. E., Chen, C., Goshima, T., Kume, K.,
1010 Hirata, D., Toda, T. and Verde, F. (2016) 'Spatial control of translation repression and
1011 polarized growth by conserved NDR kinase Orb6 and RNA-binding protein Sts5', *eLife,*
1012 5, pp. e14216.
1013 86. Panas, M. D., Ivanov, P. and Anderson, P. (2016) 'Mechanistic insights into mammalian
1014 stress granule dynamics', *Journal of Cell Biology,* 215(3), pp. 313-323.
1015 87. Parker, B. W., Gogl, G., Bálint, M., Hetényi, C., Reményi, A. and Weiss, E. L. (2020)
1016 'Ndr/Lats Kinases Bind Specific Mob-Family Coactivators through a Conserved and
1017 Modular Interface', *Biochemistry,* 59(17), pp. 1688-1700.
1018 88. Patel, A., Lee, H. O., Jawerth, L., Maharana, S., Jahnel, M., Hein, M. Y., Stoynov, S.,
1019 Mahamid, J., Saha, S., Franzmann, T. M., Pozniakovski, A., Poser, I., Maghelli, N.,
1020 Royer, L. A., Weigert, M., Myers, E. W., Grill, S., Drechsel, D., Hyman, A. A. and Alberti,
1021 S. (2015) 'A Liquid-to-Solid Phase Transition of the ALS Protein FUS Accelerated by
1022 Disease Mutation', *Cell,* 162(5), pp. 1066-77.
1023 89. Pawlik, A., Nowak, J. M., Grzanka, D., Gackowska, L., Michalkiewicz, J. and Grzanka, A.
1024 (2013) 'Hyperthermia induces cytoskeletal alterations and mitotic catastrophe in p53-
1025 deficient H1299 lung cancer cells', *Acta Histochem,* 115(1), pp. 8-15.
1026 90. Ramaswami, M., Taylor, J. P. and Parker, R. (2013) 'Altered ribostasis: RNA-protein
1027 granules in degenerative disorders', *Cell,* 154(4), pp. 727-36.

1028 91. Riback, J. A., Katanski, C. D., Kear-Scott, J. L., Pilipenko, E. V., Rojek, A. E., Sosnick, T. R.
1029 and Drummond, D. A. (2017) 'Stress-Triggered Phase Separation Is an Adaptive,
1030 Evolutionarily Tuned Response', *Cell,* 168(6), pp. 1028-1040 e19.
1031 92. Robinson, S. R., Oliver, A. W., Chevassut, T. J. and Newbury, S. F. (2015) 'The 3' to 5'
1032 Exoribonuclease DIS3: From Structure and Mechanisms to Biological Functions and
1033 Role in Human Disease', *Biomolecules,* 5(3), pp. 1515-39.
1034 93. Ross, D. T., Scherf, U., Eisen, M. B., Perou, C. M., Rees, C., Spellman, P., Iyer, V., Jeffrey,
1035 S. S., Van de Rijn, M., Waltham, M., Pergamenschikov, A., Lee, J. C., Lashkari, D.,
1036 Shalon, D., Myers, T. G., Weinstein, J. N., Botstein, D. and Brown, P. O. (2000)
1037 'Systematic variation in gene expression patterns in human cancer cell lines', *Nat Genet,*
1038 24(3), pp. 227-35.
1039 94. Sakuno, T., Araki, Y., Ohya, Y., Kofuji, S., Takahashi, S., Hoshino, S. and Katada, T. (2004)
1040 'Decapping reaction of mRNA requires Dcp1 in fission yeast: its characterization in
1041 different species from yeast to human', *J Biochem,* 136(6), pp. 805-12.
1042 95. Salat-Canela, C., Carmona, M., Martín-García, R., Pérez, P., Ayté, J. and Hidalgo, E. (2021)
1043 'Stress-dependent inhibition of polarized cell growth through unbalancing the GEF/GAP
1044 regulation of Cdc42', *Cell Reports,* 37(5), pp. 109951.
1045 96. Salat-Canela, C., Pérez, P., Ayté, J. and Hidalgo, E. (2023) 'Stress-induced cell
1046 depolarization through the MAP kinase–Cdc42 axis', *Trends in Cell Biology,* 33(2), pp.
1047 124-137.
1048 97. Satoh, R., Tanaka, A., Kita, A., Morita, T., Matsumura, Y., Umeda, N., Takada, M., Hayashi,
1049 S., Tani, T., Shinmyozu, K. and Sugiura, R. (2012) 'Role of the RNA-binding protein
1050 Nrd1 in stress granule formation and its implication in the stress response in fission
1051 yeast', *PLoS One,* 7(1), pp. e29683.
1052 98. Schindelin, J., Arganda-Carreras, I., Frise, E., Kaynig, V., Longair, M., Pietzsch, T.,
1053 Preibisch, S., Rueden, C., Saalfeld, S., Schmid, B., Tinevez, J.-Y., White, D. J.,
1054 Hartenstein, V., Eliceiri, K., Tomancak, P. and Cardona, A. (2012) 'Fiji: an open-source
1055 platform for biological-image analysis', *Nature Methods,* 9(7), pp. 676-682.
1056 99. Schwamborn, J. C. and Püschel, A. W. (2004) 'The sequential activity of the GTPases
1057 Rap1B and Cdc42 determines neuronal polarity', *Nature Neuroscience,* 7(9), pp. 923-
1058 929.
1059 100. Shiozaki, K. and Russell, P. (1996) 'Conjugation, meiosis, and the osmotic stress response
1060 are regulated by Spc1 kinase through Atf1 transcription factor in fission yeast', *Genes*
1061 *Dev,* 10(18), pp. 2276-88.

1062 101. Shiozaki, K., Shiozaki, M. and Russell, P. (1998) 'Heat stress activates fission yeast
1063 Spc1/Styl MAPK by a MEKK-independent mechanism', *Mol Biol Cell,* 9(6), pp. 1339-49.
1064 102. Singh, D., Odedra, D., Lehmann, C. and Pohl, C. (2016) 'Acute heat shock leads to cortical
1065 domain internalization and polarity loss in the C. elegans embryo', *Genesis,* 54(4), pp.
1066 220-8.
1067 103. Smith, D. A., Toone, W. M., Chen, D., Ba¨hler, J. r., Jones, N., Morgan, B. A. and Quinn, J.
1068 (2002) 'The Srk1 Protein Kinase Is a Target for the Sty1 Stress-activated MAPK in
1069 Fission Yeast*', *Journal of Biological Chemistry,* 277(36), pp. 33411-33421.
1070 104. Snell, V. and Nurse, P. (1994) 'Genetic analysis of cell morphogenesis in fission yeast--a
1071 role for casein kinase II in the establishment of polarized growth', *Embo j,* 13(9), pp.
1072 2066-74.
1073 105. Stankiewicz, T. R. and Linseman, D. A. (2014) 'Rho family GTPases: key players in
1074 neuronal development, neuronal survival, and neurodegeneration', *Frontiers in Cellular*
1075 *Neuroscience,* 8.
1076 106. Stein, V., Blank-Landeshammer, B., Müntjes, K., Märker, R., Teichert, I., Feldbrügge, M.,
1077 Sickmann, A. and Kück, U. (2020) 'The STRIPAK signaling complex regulates
1078 dephosphorylation of GUL1, an RNA-binding protein that shuttles on endosomes', *PLoS*
1079 *Genet,* 16(9), pp. e1008819.
1080 107. Sun, L., Liu, L., Song, C., Wang, Y. and Jin, Q.-w. (2024) 'Heat stress-induced activation of
1081 MAPK pathway attenuates Atf1-dependent epigenetic inheritance of heterochromatin in
1082 fission yeast', *eLife,* 13, pp. e90525.
1083 108. Toda, T., Niwa, H., Nemoto, T., Dhut, S., Eddison, M., Matsusaka, T., Yanagida, M. and
1084 Hirata, D. (1996) 'The fission yeast sts5+ gene is required for maintenance of growth
1085 polarity and functionally interacts with protein kinase C and an osmosensing MAP-kinase
1086 pathway', *J Cell Sci,* 109 (Pt 9), pp. 2331-42.
1087 109. Toone, W. M. and Jones, N. (1998) 'Stress-activated signalling pathways in yeast', *Genes*
1088 *Cells,* 3(8), pp. 485-98.
1089 110. Vaggi, F., Dodgson, J., Bajpai, A., Chessel, A., Jordan, F., Sato, M., Carazo-Salas, R. E.
1090 and Csikasz-Nagy, A. (2012) 'Linkers of cell polarity and cell cycle regulation in the
1091 fission yeast protein interaction network', *PLoS Comput Biol,* 8(10), pp. e1002732.
1092 111. van Dijk, E., Cougot, N., Meyer, S., Babajko, S., Wahle, E. and Seraphin, B. (2002)
1093 'Human Dcp2: a catalytically active mRNA decapping enzyme located in specific
1094 cytoplasmic structures', *Embo j,* 21(24), pp. 6915-24.

1095 112. Velichko, A. K., Markova, E. N., Petrova, N. V., Razin, S. V. and Kantidze, O. L. (2013)
1096 'Mechanisms of heat shock response in mammals', *Cell Mol Life Sci,* 70(22), pp. 4229-
1097 41.
1098 113. Verde, F., Mata, J. and Nurse, P. (1995) 'Fission yeast cell morphogenesis: identification of
1099 new genes and analysis of their role during the cell cycle', *J Cell Biol,* 131(6 Pt 1), pp.
1100 1529-38.
1101 114. Verde, F., Wiley, D. J. and Nurse, P. (1998) 'Fission yeast orb6, a ser/thr protein kinase
1102 related to mammalian rho kinase and myotonic dystrophy kinase, is required for
1103 maintenance of cell polarity and coordinates cell morphogenesis with the cell cycle', *Proc*
1104 *Natl Acad Sci U S A,* 95(13), pp. 7526-31.
1105 115. Versele, M. and Thevelein, J. M. (2001) 'Lre1 affects chitinase expression, trehalose
1106 accumulation and heat resistance through inhibition of the Cbk1 protein kinase in
1107 Saccharomyces cerevisiae', *Mol Microbiol,* 41(6), pp. 1311-26.
1108 116. Vichalkovski, A., Gresko, E., Cornils, H., Hergovich, A., Schmitz, D. and Hemmings, B. A.
1109 (2008) 'NDR kinase is activated by RASSF1A/MST1 in response to Fas receptor
1110 stimulation and promotes apoptosis', *Curr Biol,* 18(23), pp. 1889-95.
1111 117. Vjestica, A., Zhang, D., Liu, J. and Oliferenko, S. (2013) 'Hsp70-Hsp40 Chaperone
1112 Complex Functions in Controlling Polarized Growth by Repressing Hsf1-Driven Heat
1113 Stress-Associated Transcription', *PLOS Genetics,* 9(10), pp. e1003886.
1114 118. Wang, Z., Jiao, X., Carr-Schmid, A. and Kiledjian, M. (2002) 'The hDcp2 protein is a
1115 mammalian mRNA decapping enzyme', *Proc Natl Acad Sci U S A,* 99(20), pp. 12663-8.
1116 119. Wen, W. L., Stevenson, A. L., Wang, C. Y., Chen, H. J., Kearsey, S. E., Norbury, C. J.,
1117 Watt, S., Bahler, J. and Wang, S. W. (2010) 'Vgl1, a multi-KH domain protein, is a novel
1118 component of the fission yeast stress granules required for cell survival under thermal
1119 stress', *Nucleic Acids Res,* 38(19), pp. 6555-66.
1120 120. Wheeler, J. R., Matheny, T., Jain, S., Abrisch, R. and Parker, R. (2016) 'Distinct stages in
1121 stress granule assembly and disassembly', *Elife,* 5.
1122 121. Wilkinson, M. G., Samuels, M., Takeda, T., Toone, W. M., Shieh, J. C., Toda, T., Millar, J.
1123 B. and Jones, N. (1996) 'The Atf1 transcription factor is a target for the Sty1 stress-
1124 activated MAP kinase pathway in fission yeast', *Genes Dev,* 10(18), pp. 2289-301.
1125 122. Wu, J., Liu, T., Rios, Z., Mei, Q., Lin, X. and Cao, S. (2017) 'Heat Shock Proteins and
1126 Cancer', *Trends in Pharmacological Sciences,* 38(3), pp. 226-256.
1127 123. Yamada, H., Ohmiya, R., Yamamoto, E., Aiba, H. and Mizuno, T. (1997) 'Characterization
1128 of multicopy suppressor genes that complement a defect in the Wis1-Sty1 MAP kinase

1129 cascade involved in stress responses in Schizosaccharomyces pombe', *J Gen Appl*
1130 *Microbiol,* 43(4), pp. 209-215.
1131 124. Yang, R., Kong, E., Jin, J., Hergovich, A. and Puschel, A. W. (2014) 'Rassf5 and Ndr
1132 kinases regulate neuronal polarity through Par3 phosphorylation in a novel pathway', *J*
1133 *Cell Sci,* 127(Pt 16), pp. 3463-76.
1134 125. Zayani, Z., Matinahmadi, A., Tavakolpournegari, A. and Bidooki, S. H. (2025) 'Exploring
1135 Stressors: Impact on Cellular Organelles and Implications for Cellular Functions',
1136 *Stresses*, 5(2). DOI: 10.3390/stresses5020026.
1137 126. Zhang, L., Tang, F., Terracciano, L., Hynx, D., Kohler, R., Bichet, S., Hess, D., Cron, P.,
1138 Hemmings, B. A., Hergovich, A. and Schmitz-Rohmer, D. (2015) 'NDR functions as a
1139 physiological YAP1 kinase in the intestinal epithelium', *Curr Biol,* 25(3), pp. 296-305.
1140
1141

1127 **Main Figures and Legends**

1128

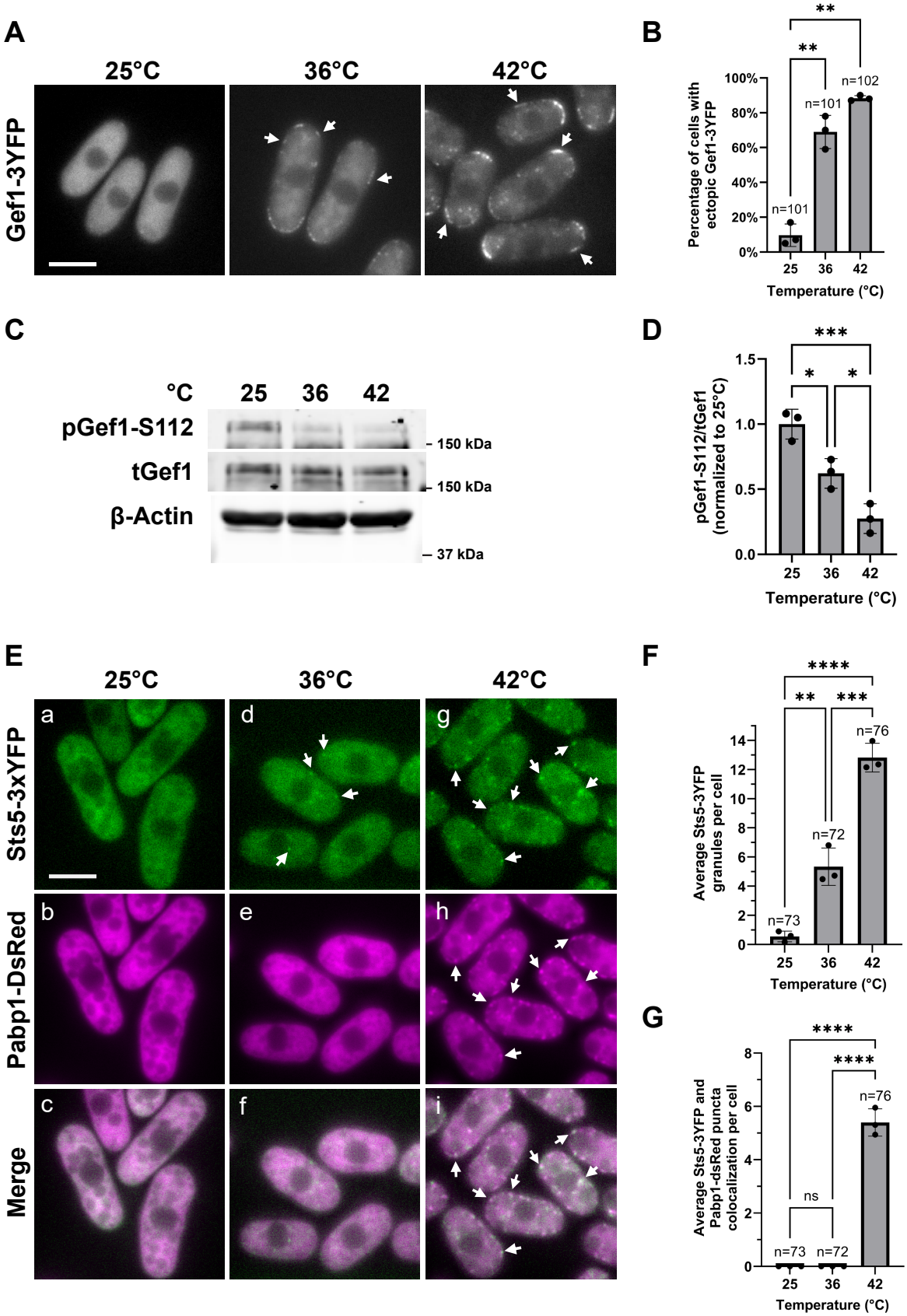
A
25°C
36°C
42°C
Gef1-3YFP
B
Percentage of cells with ectopic Gef1-3YFP
100%
80%
60%
40%
20%
0%
n=101
n=101
n=102
**
**
25
36
42
Temperature (°C)
C
°C
25
36
42
pGef1-S112
tGef1
β-Actin
150 kDa
150 kDa
37 kDa
D
pGef1-S112/tGef1 (normalized to 25°C)
1.5
1.0
0.5
0.0
***
*
*
25
36
42
Temperature (°C)
E
25°C
36°C
42°C
Sts5-3xYFP
Pabp1-DsRed
Merge
a
b
c
d
e
f
g
h
i
F
Average Sts5-3YFP granules per cell
14
12
10
8
6
4
2
0
****
**
***
n=73
n=72
n=76
25
36
42
Temperature (°C)
G
Average Sts5-3YFP and Pabp1-dsRed puncta colocalization per cell
8
6
4
2
0
****
****
ns
n=73
n=72
n=76
25
36
42
Temperature (°C)

Figure 1

1129 **Figure 1: Orb6 activity is negatively regulated by heat stress.**

1130 (A) Gef1-3YFP localizes the cell membrane upon heat exposure at 36ºC or 42ºC for 30
1131 minutes (arrows). Scale bar, 5 µm. (B) Quantification of percentage of cells that display
1132 ectopic Gef1-3YFP localization from A based on three independent experiments. Data
1133 presented as mean ± SD, *p* values are determined by one-way ANOVA with Tukey's HSD
1134 test $p \leq 0.01$, **. n = number of cells quantified. (C) Orb6 activity, as measured by Gef1-
1135 S112 phosphorylation, decreases after 30 minutes at 36ºC or 42ºC. (D) Quantification of
1136 pGef1-S112/tGef1 from C upon temperature stress exposure based on three independent
1137 experiments. Data are presented as in B, $p \leq 0.05$, *; $p \leq 0.001$, ***. (E) *Sts5-3xGFP*
1138 *pabp1-DsRed* cells were exposed to 36ºC or 42ºC for 30 minutes. At 36ºC, Sts5-3xGFP
1139 formed cytoplasmic puncta (d, arrows) but no stress granule formation was visible (f). At
1140 42ºC, Sts5 partially co-localized with the stress granule marker Pabp1-DsRed (g-i,
1141 arrows). Scale bar, 5 µm. (F) Quantification of average number of Sts5 puncta present in
1142 each cell from E based on three independent experiments. Data are presented as in B, p
1143 ≤ 0.01, **; $p \leq 0.001$, ***, $p \leq 0.0001$, ****. n = number of cells quantified. (G) Quantification
1144 of average number of Sts5 puncta that colocalized by stress granule marker Pabp1 in
1145 each cell from E based on three independent experiments. Data are presented as in B, p
1146 ≤ 0.0001, ****. n = number of cells quantified.
1147

1148

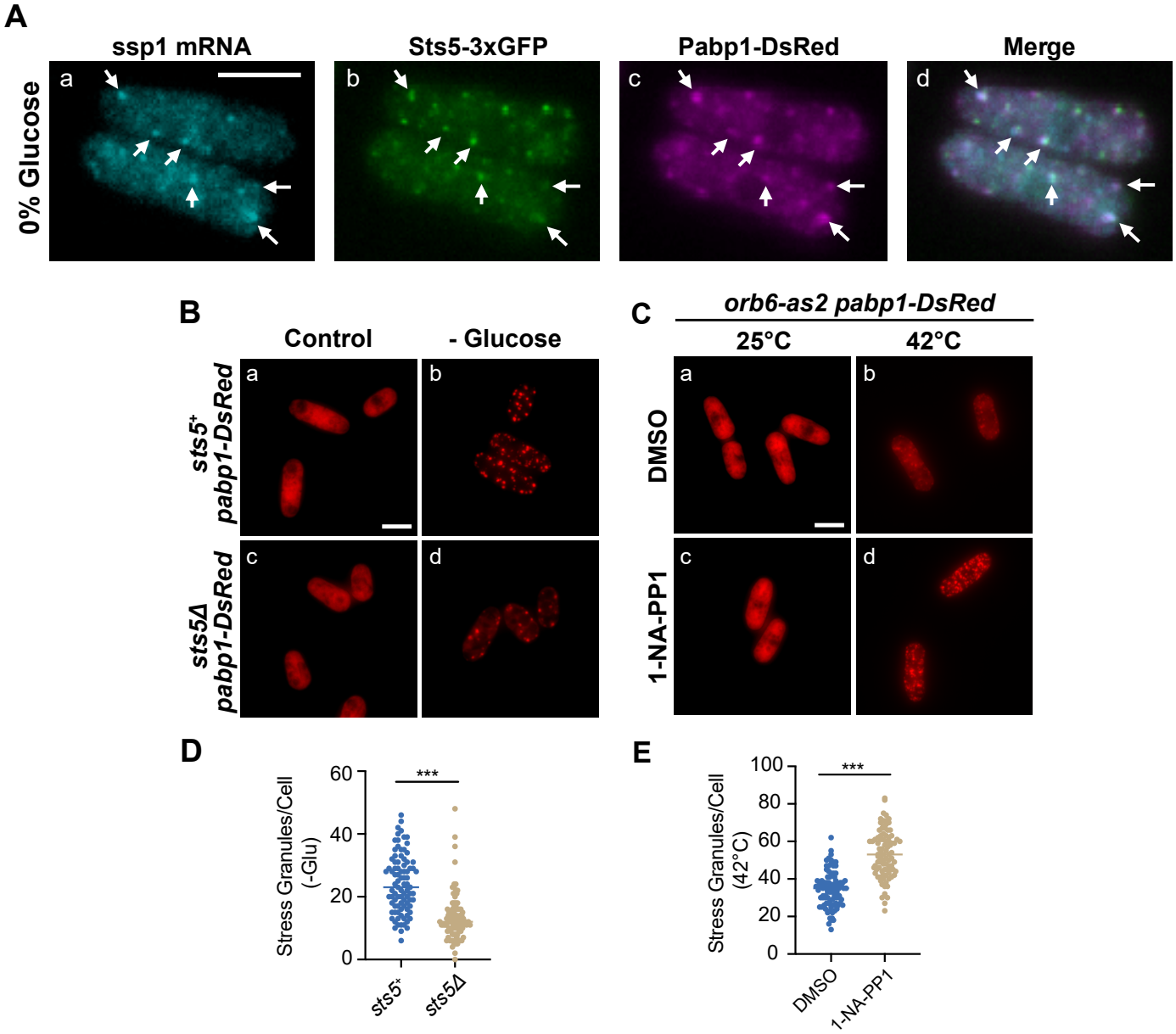
A
ssp1 mRNA
Sts5-3xGFP
Pabp1-DsRed
Merge
0% Glucose
a
b
c
d
B
Control
- Glucose
sts5+ pabp1-DsRed
sts5Δ pabp1-DsRed
C
orb6-as2 pabp1-DsRed
25°C
42°C
DMSO
1-NA-PP1
D
Stress Granules/Cell (-Glu)
60
40
20
0
***
sts5+
sts5Δ
E
Stress Granules/Cell (42°C)
100
80
60
40
20
0
***
DMSO
1-NA-PP1

Figure 2

1149 **Figure 2: Orb6 and Sts5 regulate stress granule formation.**

1150 (A) RNA FISH visualization of ssp1 mRNA in fixed cells cultured for 20 minutes in minimal
1151 medium containing 0% glucose. Hybridization of RNA was performed with 20-mer DNA
1152 oligonucleotides (Stellaris) labeled with Quasar 705 fluorochromes. ssp1 mRNA co-
1153 localized with Sts5-3xGFP and the stress granule marker Pabp1-DsRed (arrows). Images
1154 are deconvolved projections from Z-stacks (12 slices) separated by a step size of 0.3 μM
1155 (Bar = 5 μM). (B) *pabp1-DsRed* and *sts5Δ pabp1-DsRed* cells were cultured in EMM
1156 medium with (a, c) or without (b, d) glucose for 20 minutes. In untreated controls, the
1157 stress granule marker Pabp1-DsRed remained diffuse throughout the cytoplasm.
1158 Following glucose deprivation, *sts5Δ* cells formed less stress granules than the control
1159 (b, d). Representative images are deconvolved projections from Z-stacks separated by a
1160 step size of 0.3 μM (Bar = 5 μM). (C) Inhibition of Orb6 primes cells for the formation of
1161 stress granules. *orb6-as2 pabp1-DsRed* cells were cultured in minimal medium
1162 containing adenine, and 15 minutes prior to heat shock 1-NA-PP1 inhibitor was added,
1163 or DMSO for controls. In cells maintained at 25ºC, Pabp1-DsRed remained diffuse within
1164 the cytoplasm (a, c). However, in cells that were heat shocked for 20 minutes at 42ºC (15
1165 minutes post addition of 1-NA-PP1), there was an increase in stress granule formation
1166 compared to the DMSO control (b, d). Representative images are deconvolved
1167 projections from Z-stacks separated by a step size of 0.3 μM (Bar = 5 μM). (D) The
1168 number of stress granules were quantified for experiment represented in B (n=90
1169 cells/strain/condition total, performed in biological triplicate), and there was a statistically
1170 significant decrease in stress granule formation for the *sts5Δ* mutant as compared to the
1171 control (***$p<0.001$; unpaired t-test). (E) The increase in stress granule formation from C
1172 was statistically significant and performed in biological triplicates (n=90
1173 cells/strain/condition total; ***$p<0.001$, unpaired t-test).
1174

1175

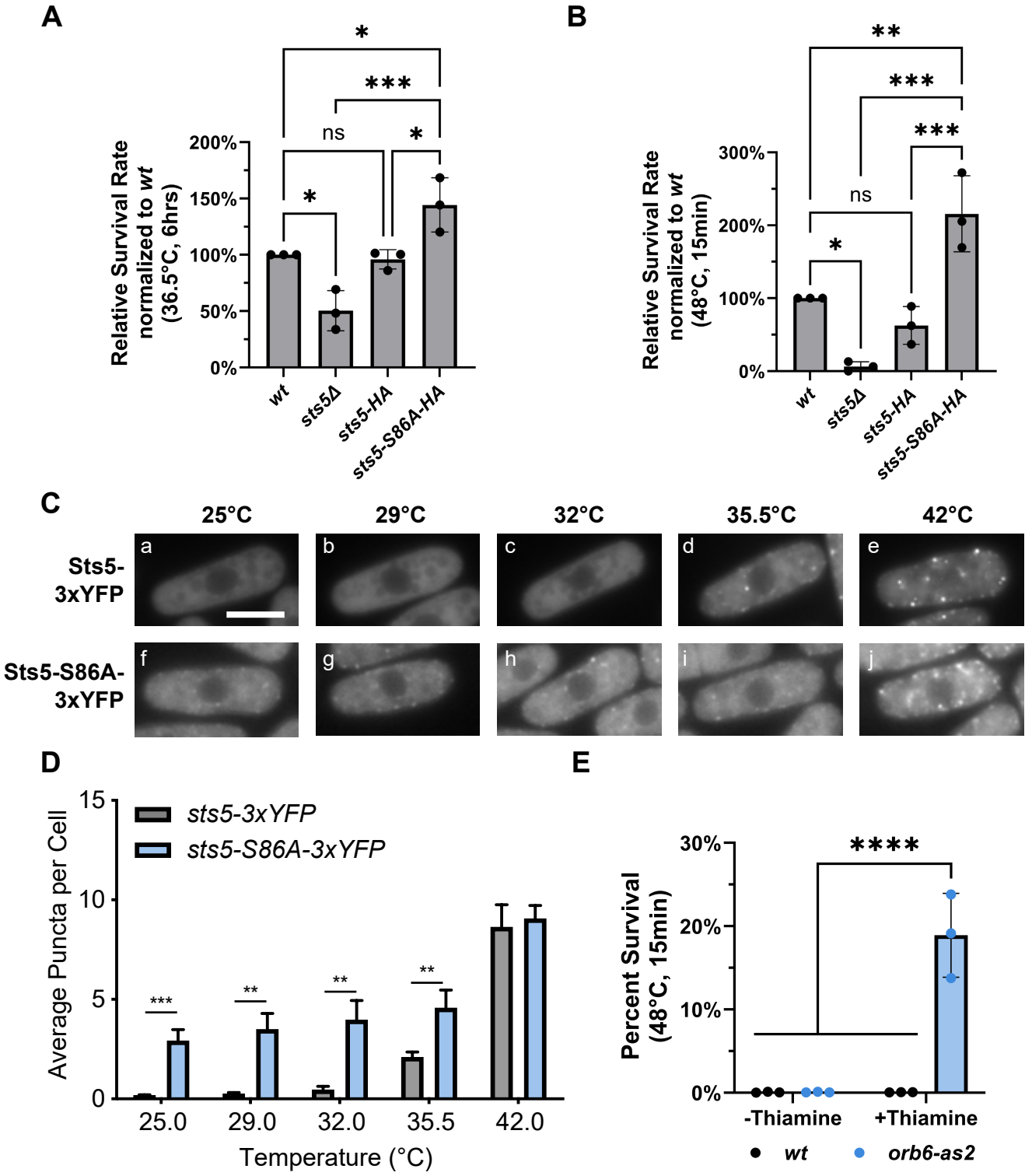
A
Relative Survival Rate normalized to wt (36.5°C, 6hrs)
200%
150%
100%
50%
0%
*
***
ns
*
*
wt
sts5Δ
sts5-HA
sts5-S86A-HA
B
Relative Survival Rate normalized to wt (48°C, 15min)
300%
200%
100%
0%
**
***
***
ns
*
wt
sts5Δ
sts5-HA
sts5-S86A-HA
C
25°C
29°C
32°C
35.5°C
42°C
Sts5-3xYFP
Sts5-S86A-3xYFP
a
b
c
d
e
f
g
h
i
j
D
Average Puncta per Cell
15
10
5
0
sts5-3xYFP
sts5-S86A-3xYFP
***
**
**
**
25.0
29.0
32.0
35.5
42.0
Temperature (°C)
E
Percent Survival (48°C, 15min)
30%
20%
10%
0%
****
-Thiamine
+Thiamine
wt
orb6-as2

Figure 3

1176 **Figure 3: Orb6 and Sts5 modulate survival following heat stress.**

1177 (A) *Wild-type, sts5Δ, sts5-HA,* and *sts5-S86A-HA* cells were grown for 6 hours at either
1178 25ºC or 36.5ºC. Following prolonged heat stress at 36.5ºC, s*ts5Δ* cells displayed
1179 decreased survival compared to wild type, whereas *sts5-S86A-HA* showed increased
1180 survival compared to the *sts5-HA* control. Data are presented as mean ± SD, p values
1181 determined by one-way ANOVA with Tukey's HSD test p ≤ 0.05, *; p ≤ 0.01, **; p ≤ 0.001,
1182 ***. (B) The experiment in A was repeated, but cells were instead incubated for 15 minutes
1183 at 48ºC temperature, while untreated controls were incubated at 25ºC. Again, *sts5Δ* cells
1184 exhibit decreased survival, whereas the *sts5-S86A-HA* mutant exhibited increased
1185 survival. Data are presented as mean ± SD, p values determined by one-way ANOVA
1186 with Tukey's HSD test p ≤ 0.05, *; p ≤ 0.001, ***. (C) In the *sts5-S86A-3xYFP* mutant, the
1187 number of Sts5 granules were increased at temperatures in which the *sts5-3xYFP* control
1188 did not form granules. (D) Quantification from results obtained in C. There is a statistically
1189 significant increase in average puncta per cell for the *sts5-S86A-3xYFP* strain as
1190 compared to the control for cells incubated between 25ºC and 35.5ºC Data are presented
1191 as mean ± SD, p values determined by two-way ANOVA with Tukey's HSD test p ≤ 0.01,
1192 **; p ≤ 0.001, ***. n=60 cells/strain performed in biological triplicates (E) *Wild-type* and
1193 *orb6-as2* strains were cultured in the presence (+Thiamine) or absence of thiamine (-
1194 Thiamine), heat shocked, and plated. Inhibition of Orb6 results in a 17-fold increase in
1195 survival as compared to the untreated control. Data are presented as mean ± SD, p values
1196 determined by two-way ANOVA with Tukey's HSD test p ≤ 0.0001, ****.
1197

1198

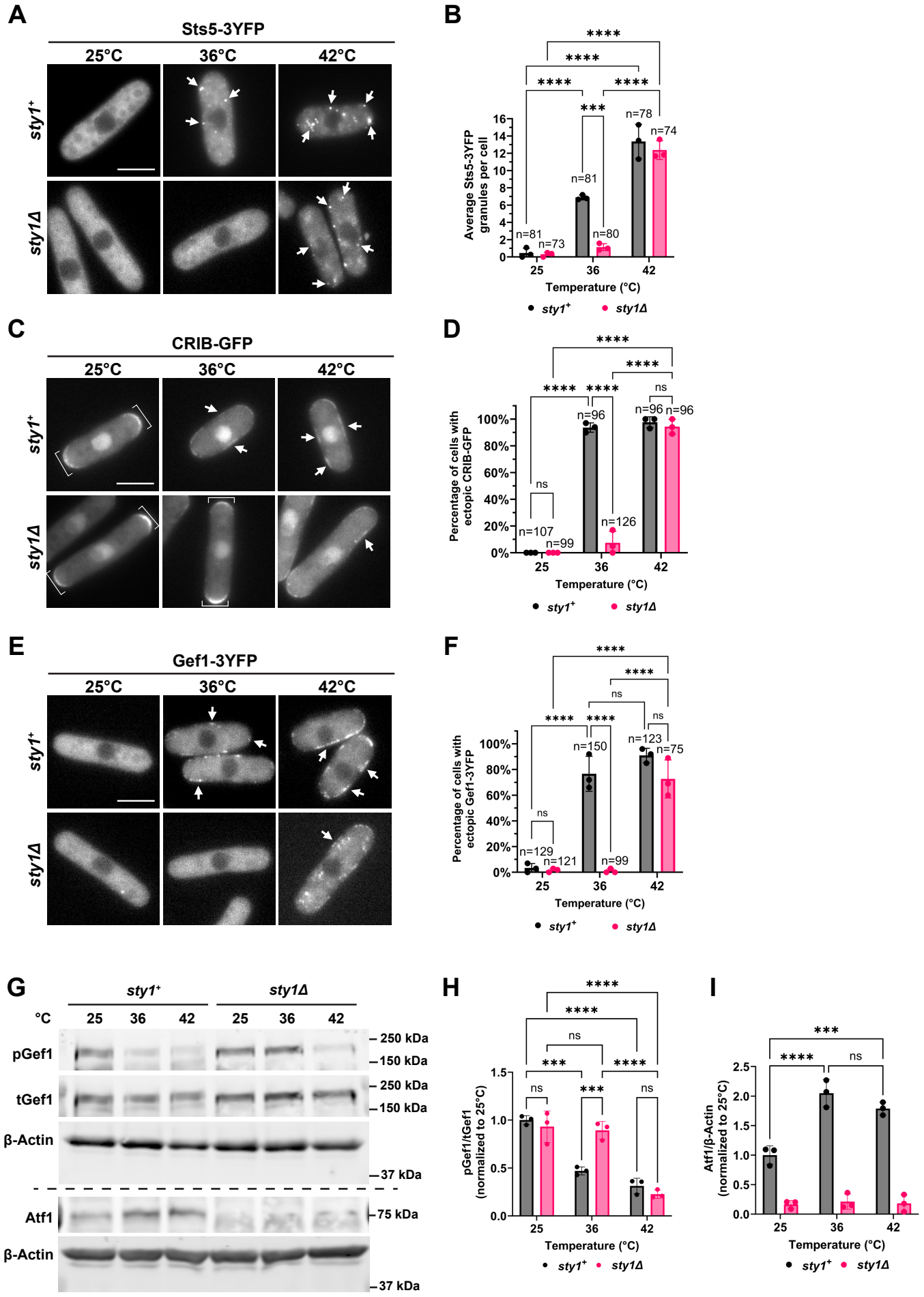
A
Sts5-3YFP
25°C
36°C
42°C
sty1+
sty1Δ
B
Average Sts5-3YFP granules per cell
Temperature (°C)
n=81
n=73
n=81
n=80
n=78
n=74
****
***
sty1+
sty1Δ
C
CRIB-GFP
25°C
36°C
42°C
sty1+
sty1Δ
D
Percentage of cells with ectopic CRIB-GFP
Temperature (°C)
n=107
n=99
n=96
n=126
n=96
n=96
ns
****
sty1+
sty1Δ
E
Gef1-3YFP
25°C
36°C
42°C
sty1+
sty1Δ
F
Percentage of cells with ectopic Gef1-3YFP
Temperature (°C)
n=129
n=121
n=150
n=99
n=123
n=75
ns
****
sty1+
sty1Δ
G
sty1+
sty1Δ
°C
25
36
42
25
36
42
pGef1
tGef1
β-Actin
Atf1
β-Actin
250 kDa
150 kDa
250 kDa
150 kDa
37 kDa
75 kDa
37 kDa
H
pGef1/tGef1 (normalized to 25°C)
Temperature (°C)
ns
***
****
sty1+
sty1Δ
I
Atf1/β-Actin (normalized to 25°C)
Temperature (°C)
***
****
ns
sty1+
sty1Δ

Figure 4

1199 **Figure 4: The distribution of Sts5, Gef1, and active Cdc42 is temperature sensitive**
1200 **and is modulated by Sty1 in a temperature specific manner.**

1201 (A) Sts5-3YFP forms puncta after 30 minutes at 36°C and 42°C (arrows). In the absence
1202 of *sty1,* Sts5-3YFP only clusters at 42°C. Images are a max projection Z-stack of 6 images
1203 separated by a step-size of 0.3 µm. Scale bar, 5 µm. (B) Quantification of average number
1204 of Sts5 puncta present in each cell from A based on three independent experiments. Data
1205 are presented as mean ± SD, p values determined by two-way ANOVA with Tukey's HSD
1206 test p ≤ 0.001, ***; p ≤ 0.0001, ****. n = number of cells quantified. (C) Active Cdc42 forms
1207 exploratory patches upon exposure to 36°C and 42°C when *sty1* is present but only forms
1208 patches at 42°C when *sty1* is absent (arrows). Active Cdc42 is localized at the cell tips in
1209 control cells at 25°C and in *sty1Δ* cells at 25°C and 36°C (brackets) Images are a max
1210 projection Z-stack of 6 images separated by a step-size of 0.3 µm. Scale bar, 5 µm. (D)
1211 Quantification of percentage of cells that display ectopic CRIB-GFP localization from C
1212 based on three independent experiments. Data presented as in D, p ≤ 0.0001, ****. n =
1213 number of cells quantified. (E) Gef1-3YFP localizes to the cell membrane at 36°C and
1214 42°C (arrows). Loss of *sty1* leads to Gef1-3YFP localization to the cell membrane only at
1215 42°C. Scale bar, 5 µm. (F) Quantification of percentage of cells that display ectopic Gef1-
1216 3YFP localization from B based on three independent experiments. Data presented as in
1217 D, p ≤ 0.0001, ****. n = number of cells quantified. (G) Gef1-S112 phosphorylation by
1218 Orb6 decreases after 30 minutes at 36°C or 42°C. In *sty1Δ* deletion cells, pGef1-S112
1219 remains constant at 36°C but decreases at 42°C. Atf1 levels increase upon exposure to
1220 36°C or 42°C for 30 minutes in control cells. β-Actin was used as a loading control. (H)
1221 Quantification of pGef1-S112/tGef1 from A upon temperature stress exposure in control
1222 or *sty1Δ* deletion mutant cells based on three independent experiments. Data are
1223 presented as mean ± SD, *p* values are determined by two-way ANOVA with Tukey's HSD
1224 test p ≤ 0.001, ***; p ≤ 0.0001, ****. (I) Quantification of Atf1/Actin from A upon
1225 temperature stress in control or *sty1Δ* deletion mutant cells based on three independent
1226 experiments. Data are presented as mean ± SD, *p* values are determined by two-way
1227 ANOVA with Tukey's HSD test p ≤ 0.001, ***; p ≤ 0.0001, ****.
1228

1229

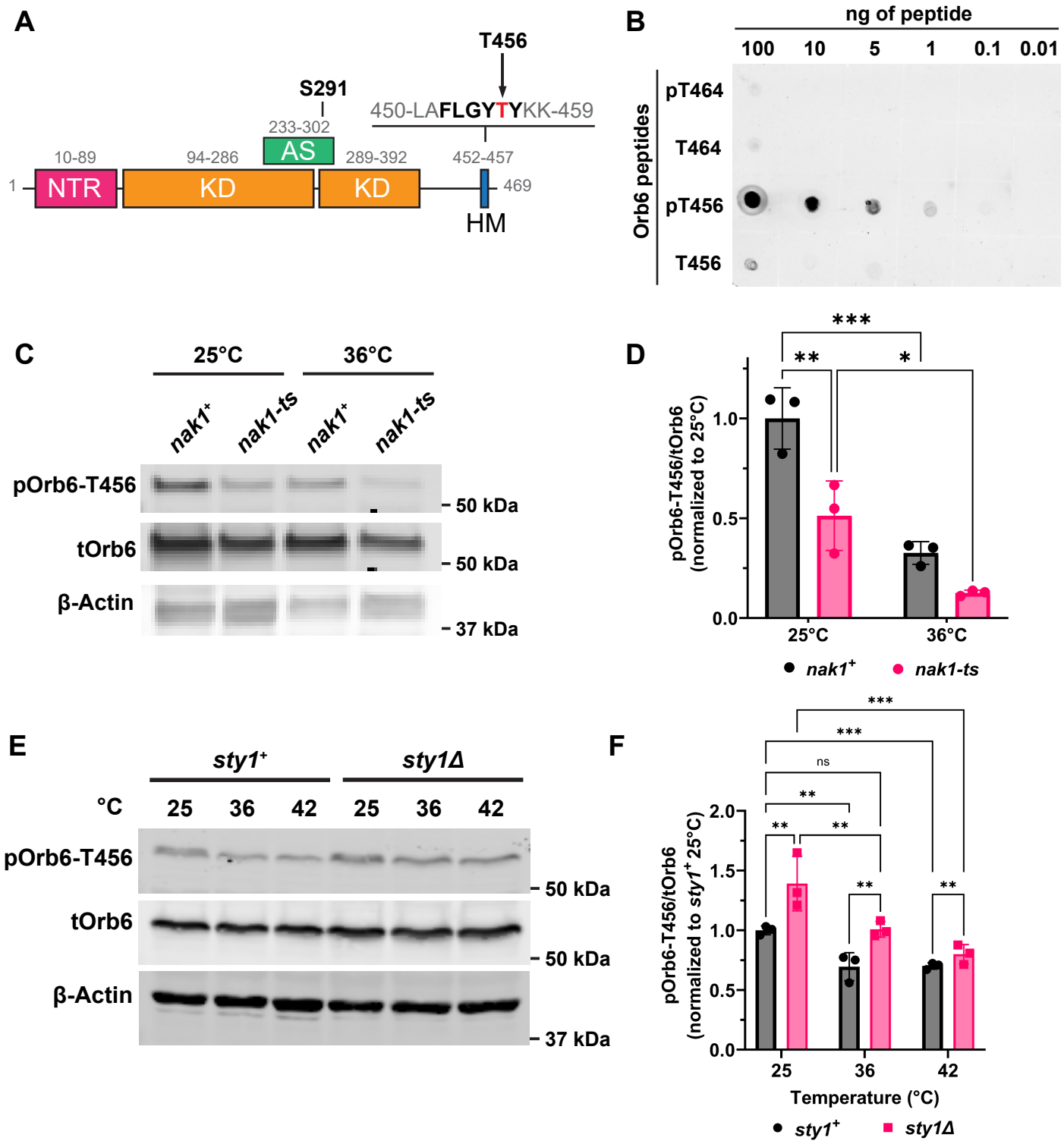
A
T456
S291
450-LAFLGYTYKK-459
233-302
AS
10-89
94-286
289-392
452-457
1
NTR
KD
KD
469
HM
B
ng of peptide
100
10
5
1
0.1
0.01
Orb6 peptides
pT464
T464
pT456
T456
C
25°C
36°C
nak1+
nak1-ts
nak1+
nak1-ts
pOrb6-T456
tOrb6
β-Actin
50 kDa
50 kDa
37 kDa
D
***
**
*
pOrb6-T456/tOrb6
(normalized to 25°C)
1.0
0.5
0.0
25°C
36°C
nak1+
nak1-ts
E
sty1+
sty1Δ
°C
25
36
42
25
36
42
pOrb6-T456
tOrb6
β-Actin
50 kDa
50 kDa
37 kDa
F
***
***
ns
**
**
**
**
**
pOrb6-T456/tOrb6
(normalized to sty1+ 25°C)
2.0
1.5
1.0
0.5
0.0
25
36
42
Temperature (°C)
sty1+
sty1Δ

Figure 5

1230 **Figure 5: The phosphorylation state of the Orb6 C-terminal hydrophobic motif is**
1231 **temperature sensitive.**

1232 (A) Protein domain map of Orb6 kinase highlighting two phosphosites: S291 in the
1233 activation segment and T456 in the hydrophobic motif. NTR:N-terminal region; KD: kinase
1234 domain; AS: activation segment; HM: hydrophobic motif. (B) Dot plot showing specificity
1235 of phosphor-Orb6-T456 antibody. (C) Orb6-456 phosphorylation decreases when
1236 temperature sensitive mutant of *nak1* (*nak1-ts)* is exposed to restrictive temperature for
1237 3 hours. (D) Quantification of pOrb6-T456/tOrb6 from C based on three independent
1238 experiments. Data are presented as mean ± SD, *p* values are determined by two-way
1239 ANOVA with Tukey's HSD test $p \leq 0.05$, *; $p \leq 0.01$, **; $p \leq 0.001$, ***. (E) Orb6-T456
1240 phosphorylation decreases after 30 minutes at 36°C or 42°C in control or *sty1Δ* deletion
1241 mutant cells. Orb6-T456 phosphorylation is higher in *sty1Δ* mutants. β-Actin was used as
1242 a loading control. (F) Quantification of pOrb6-T456/tOrb6 from A based on three
1243 independent experiments. Data are presented as mean ± SD, *p* values are determined
1244 by two-way ANOVA with Tukey's HSD test $p \leq 0.01$, **; $p \leq 0.001$, ***.
1245

1246

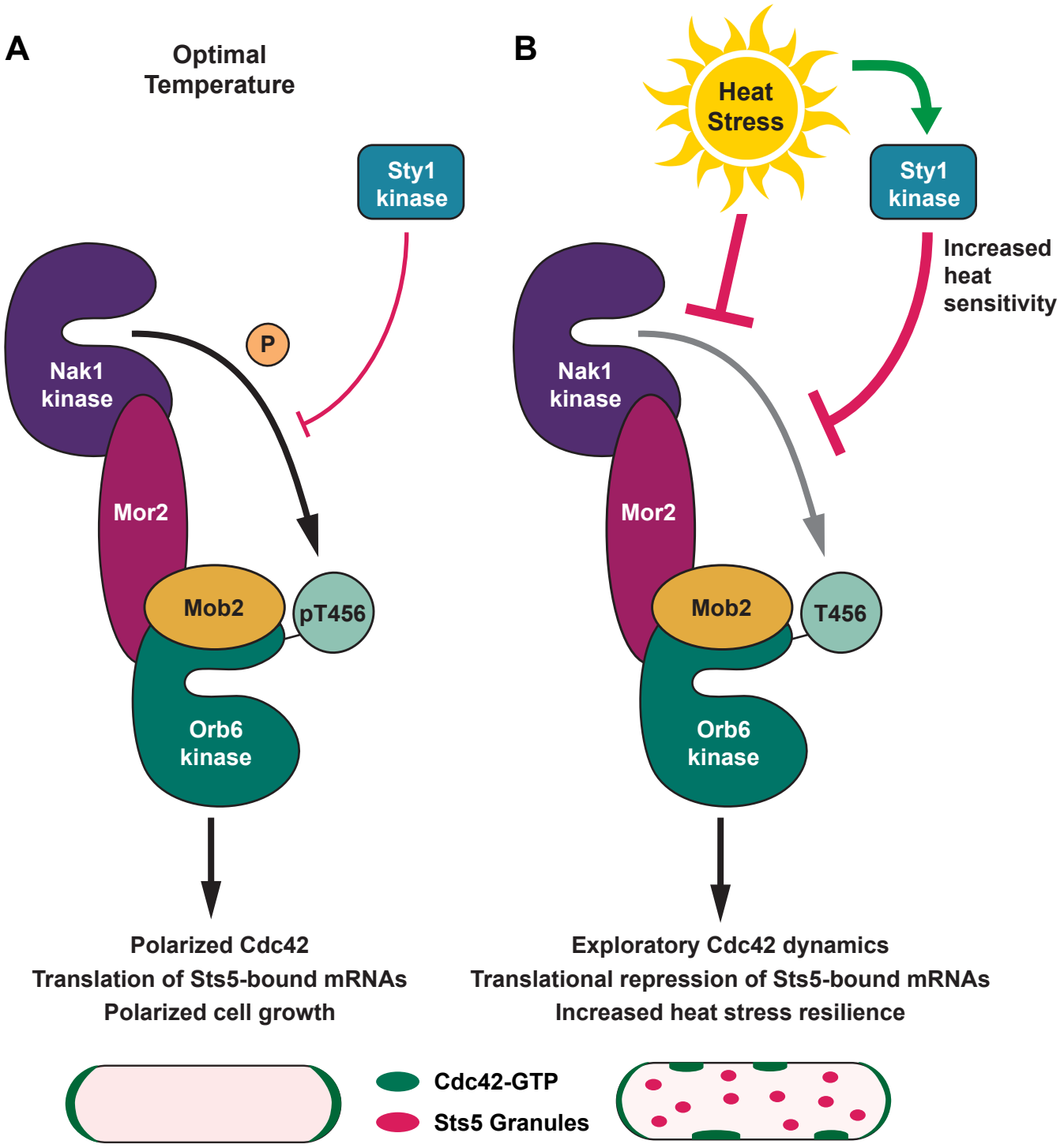
A
Optimal Temperature
Sty1 kinase
P
Nak1 kinase
Mor2
Mob2
pT456
Orb6 kinase
Polarized Cdc42
Translation of Sts5-bound mRNAs
Polarized cell growth
B
Heat Stress
Sty1 kinase
Increased heat sensitivity
Nak1 kinase
Mor2
Mob2
T456
Orb6 kinase
Exploratory Cdc42 dynamics
Translational repression of Sts5-bound mRNAs
Increased heat stress resilience
Cdc42-GTP
Sts5 Granules

Figure 6

1247 **Figure 6: Regulation of NDR kinase Orb6 by temperature and MAP kinase Sty1.**

1248 (A) Orb6 kinase activity at optimal, not stressful temperatures (25°C) promotes the
1249 canonical Cdc42 polarity module (via regulation of RNA Binding protein Sts5), and
1250 polarized cell growth. (B) Upon heat stress, MAP kinase Sty1 is strongly activated and
1251 inhibits Orb6 kinase activity, thereby promoting exploratory Cdc42 dynamics, Sts5
1252 granule assembly, translational repression of Sts5-associated mRNAs, and increased
1253 heat stress resilience. The induction of exploratory Cdc42 dynamics also involves direct
1254 phosphorylation of Orb6 substrates by Sty1 Kinase (see Discussion). Inhibition of Orb6
1255 kinase activity during heat stress also engages Sty1-independent regulatory
1256 mechanisms, likely affecting other components of the MOR (Morphogenesis Orb6
1257 network) pathway. The activity of MAP kinase Sty1 lowers the threshold temperature that
1258 triggers Orb6 inhibition, thereby rendering Orb6 more temperature sensitive and
1259 promoting thermotolerance.
1260
1261